# Supporting Information for

# Solution processable *meso*-triarylamine functionalized porphyrins with high mobility and ON/OFF ratio in bottom-gated OFETs

Komal Kurlekar,[†] AnshikaAnjali,[†] Srinita Sonalin,[†]Predhanekar Mohamed Imran,[‡]

Samuthira Nagarajan*[†]

[†]Department of Chemistry, Central University of Tamil Nadu, Thiruvarur- 610 005, India

*Email: snagarajan@cutn.ac.in

[‡]Department of Chemistry, Islamiah College, Vaniyambadi - 635 752, India

# Table of content

## Materials and methods

Triphenylamine, $POCl_3$, tetrakis(triphenylphosphine)palladium, and all the boronic acids (thiophene-3-boronic acid, benzeneboronic acid, 3-fluoroboronic acid, 4- methoxyphenylboronic acid, 3-trifluoromethylboronic acid), pyrrole, *p*-formaldehyde,indium trichloride ($InCl_3$),2,3-dichloro-5,6-dicyano-1,4-benzoquinone(DDQ),trifluoroacetic acid (TFA), were used as purchased from the commercial sources. N, N-Dimethylformamide (DMF) and triethylamine used were anhydrous. All the other solvents (AR grade) were used as received. $^1H$ NMR and $^{13}C$ NMR were recorded in Bruker 400 MHz spectrometer in $CDCl_3$. Chemical shifts are reported against TMS. Absorption spectra of compounds were recorded by JASCO UV-NIR spectrophotometer. Fluorescence measurements were obtained from Perkin Elmer Spectrofluorimeter LS55. Thermal studies carried out in TA thermal analyzer. Electrochemical studies were done with CH Instruments: Electrochemical workstation (CHI 6035D). High-resolution mass spectra were recorded in ThermoExactivePlus UHPLC-MS. Keithley semiconductor parameter analyzer 4200 SCS was employed to determine the organic field-effect transistor behavior (OFET) of the compounds.

### Experimental procedure

**4-(Bis(4-iodophenyl)amino)benzaldehyde (2):**

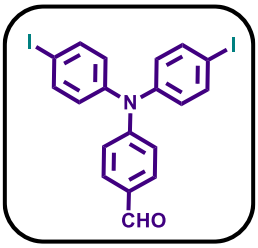


Compound **1:** DMF (2 ml, 25.9 mmol) was transferred into 100 ml RB and maintained at 0°C. To this $POCl_3$ (1.9 ml, 20.4 mmol) was added dropwise for 20 min. Triphenylamine (TPA) (1 g, 4.0 mmol) was added at room temperature, during which the solution color changed to pale yellow, and stirred for 1 h. The reaction mixture was then heated to 45°C and stirred for an additional 2 h. The resultant mixture was poured into an ice bath and neutralized with sodium bicarbonate. The solution was extracted with dichloromethane and distilled water.[1] The pale yellow solid (1 g, 92 %) was purified by column chromatography using silica gel (v/v hexane-ethyl acetate: 9/1).

Compound **2:** Under rapid stirring, compound **1** (1 g, 3.6 mmol) was dissolved in glacial acetic acid (10 ml). KI (1.2 g, 7.3 mmol) and $KIO_3$ (2.3 g, 10.9 mmol) were added to the reaction mixture and stirred for 6 h at 70°C. After cooling, the reaction was quenched with sodium thiosulphate solution. Solid yellow powder formed was filtered and washed with water. The pure product (1.8 g, 98 %) was purified by column chromatography using silica gel (v/v hexane-ethyl acetate = 9/1).

**General procedure for Suzuki coupling reaction (3):**

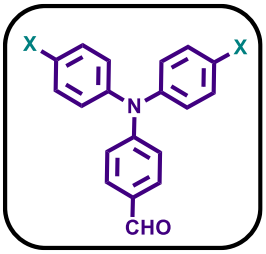


Compound **2** was dissolved in THF, to the solution 10 mol % of $Pd(PPh_3)_4$ was added at room temperature and stirred for 10 min under nitrogen atmosphere. Aqueous solution of $Na_2CO_3$ (2 M) was added and stirred for 20 min at room temperature. The temperature was raised to 65°C followed by addition of appropriate boronic acid and stirred for 8 h. The reaction mixture was extracted with ethyl acetate and distilled water.[2] The pure yellow solid was purified by column chromatography using silica gel (v/v hexane-ethyl acetate).

**Di(1*H*-pyrrol-2-yl)methane (4):**

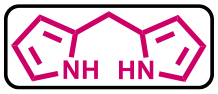


A mixture of paraformaldehyde and freshly distilled pyrrole (35 ml, 504.4 mmol) was taken into a 250 ml RB and degassed with nitrogen for 10 min at RT. The temperature was raised to 55°C for 10 min under nitrogen atmosphere and $InCl_3$ (0.1 g, 0.5 mmol) was added subsequently. The reaction mixture was stirred for 2 h 30 min at the same temperature and then cooled to RT followed by the addition of powdered NaOH (0.6 g, 15.2 mmol) to quench the reaction mixture and stirred for further 1 h.[3] The mixture was filtered and the filtrate was concentrated in vacuum. Off white solid was purified by column chromatography using silica gel (v/v hexane-DCM = 1/1).White solid. Yield: 56%. $^1$H NMR (400 MHz, $CDCl_3$): δ (ppm) 7.797 (s, 2H), 6.635 (s, 2H), 6.145 (s, 2H), 6.032 (s, 2H), 3.956 (s, 2H). $^{13}$C NMR ($CDCl_3$, 100 MHz): δ (ppm) 117.46, 108.31, 106.56, 26.35. HRMS (ESI) m/z calcd for $C_9H_{10}N_2$ 146.084, found 145.075.

**General procedure for porphyrin 5:**

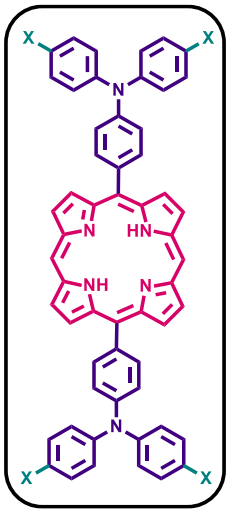


A mixture of compound **3** (1 g, 1.9 mmol) and **4** (0.6 g, 3.8 mmol) was dissolved in $CH_2Cl_2$ (460 ml) solvent, then degassed with nitrogen at RT.Trifluoroaceticacid (53 µl, 0.69 mmoles) dissolved in 50 ml DCM was added dropwise and stirred for 7 hr. Further DDQ (0.783 g, 3.45 mmoles) was added and stirred for additional 1hr. Finally the reaction mixture was basified with triethylamine (2 ml) and solvent removed under vacuum.[4] Purple powder was purified by column chromatography (v/v hexane-DCM = 1/1).

**4-(Bis(4-(thiophen-3-yl)phenyl)amino)benzaldehyde, 3a:**

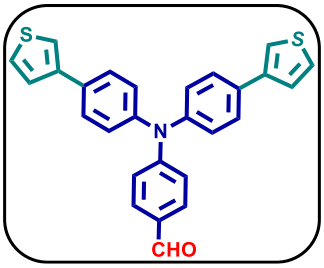


Yellow solid. Yield: 90%. $^1$H NMR (400 MHz, $CDCl_3$): δ (ppm) 9.820 (s, 1H), 7.690 (d, J = 8.8 Hz, 2H), 7.560 (d, J = 8.4 Hz, 2H), 7.427-7.320 (m, 6H), 7.208-7.176 (m, 6H), 7.064 (d, J = 8.8 Hz, 2H). $^{13}$C NMR ($CDCl_3$, 100 MHz): δ (ppm) 190.48, 153.20, 146.06, 145.12, 141.12, 141.47, 132.60, 131.36, 129.81, 129.75, 129.29, 127.65, 126.44, 126.35, 126.34, 126.13, 125.23, 125.14, 120.14, 119.65, 119.36.HR-MS (ESI) m/z calcd for $C_{27}H_{19}NOS_2$[M+H] 437.0908, found 437.0863.

**4-(Di([1,1'-biphenyl]-4-yl)amino)benzaldehyde, 3b:**

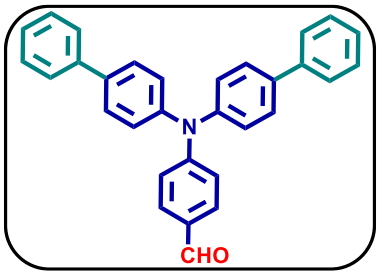


Yellow solid. Yield: 82 %. $^{1}$H NMR (400 MHz, $CDCl_3$): δ (ppm) 9.842 (s, 1H), 7.731 (d, J = 8.8 Hz, 2H), 7.590 (dd, 8H), 7.44 (t, 4H), 7.36 (t, 2H), 7.27 (d, J = 8.4 Hz, 4H), 7.148 (d, J = 8.8 Hz, 2H). $^{13}$C NMR ($CDCl_3$, 100 MHz): δ (ppm) 190.51, 153.12, 145.35, 140.23, 137.87, 131.39, 129.49, 128.88, 128.37, 127.35, 126.88, 126.35, 120.04.HRMS (ESI) m/z calcd for $C_{31}H_{23}NO$ [M+H] 426.1858, found 426.1852.

**4-(Bis(4'-fluoro-[1,1'-biphenyl]-4-yl)amino)benzaldehyde 3c:**

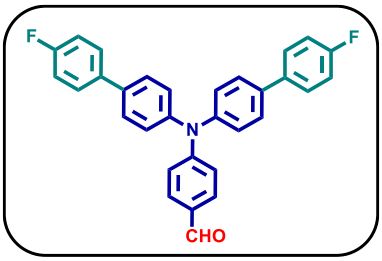


Yellow solid. Yield: 75%. $^{1}$H NMR (400 MHz, $CDCl_3$): δ (ppm) 9.846 (s, 1H), 7.732 (d, J = 8.4 Hz, 2H), 7.567-7.519 (m, 8H), 7.267 (d, J = 1.6 Hz, 2H), 7.158-7.118 (m, 6H). $^{13}$C NMR ($CDCl_3$, 100 MHz): δ (ppm) 190.48, 163.71, 161.26, 153.01, 145.34, 136.89, 136.37, 136.34, 128.24, 126.36, 120.12, 115.88, 115.66.HRMS (ESI) m/z calcd for $C_{33}H_{21}NOF_6$ [M+H] 462.166, found 462.164.

**4-(Bis(4'-methoxy-[1,1'-biphenyl]-4-yl)amino)benzaldehyde 3d:**

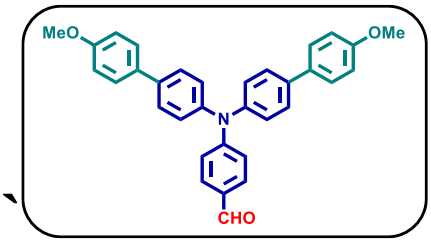


Yellow solid. Yield: 85%. $^{1}$H NMR (400 MHz, $CDCl_3$): δ (ppm) 9.829 (s, 1H), 7.715 (d, J = 8.8 Hz, 2H), 7.534 (d, J = 7.2 Hz, 8H), 7.246 (d, J = 8.4 Hz, 4H), 7.120 (d, J = 8.8 Hz, 2H), 6.986 (d, J = 8.8 Hz, 4H), 3.861 (s, 6H). $^{13}$C NMR ($CDCl_3$, 100 MHz): δ (ppm) 190.48, 159.19, 153.23, 144.73, 137.56, 132.78, 131.38, 129.22, 127.91, 127.87, 126.44, 119.63, 114.30. HRMS (ESI) m/z calcdfor $C_{33}H_{27}NO_3$ [M+H] 486.2069, found 486.2072.

**4-(Bis(3'-(trifluoromethyl)-[1,1'-biphenyl]-4-yl)amino)benzaldehyde 3e:**

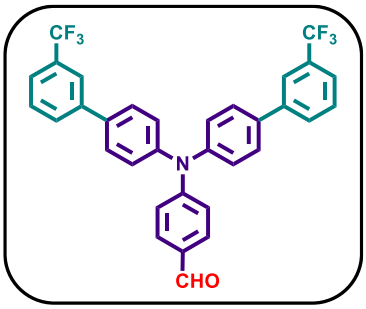


Yellow solid. Yield: 90%. $^{1}$H NMR (400 MHz, $CDCl_3$): δ (ppm) 9.870 (s, 1H), 7.837 (s, 1H), 7.781-7.747 (m, 4H), 7.623-7.551 (m, 8H), 7.294 (d, J = 8.8 Hz, 4H), 7.173 (d, J = 8.4 Hz, 2H). $^{13}$C NMR ($CDCl_3$, 100 MHz): δ (ppm) 190.50, 152.77, 146.06, 142.02, 136.30, 135.23, 131.77, 131.45, 131.41, 131.13, 130.81, 130.25, 130.11, 130.05, 129.37, 128.52, 128.22, 127.72, 127.67, 127.61, 126.31, 125.51, 124.02, 123.98, 123.73, 123.69, 123.65, 123.61, 122.80, 120.69, 120.10.HRMS (ESI) m/z calcd for $C_{33}H_{21}NOF_6$ [M+H] 562.1606, found 562.157.

**<u>Compound 5a</u>:**

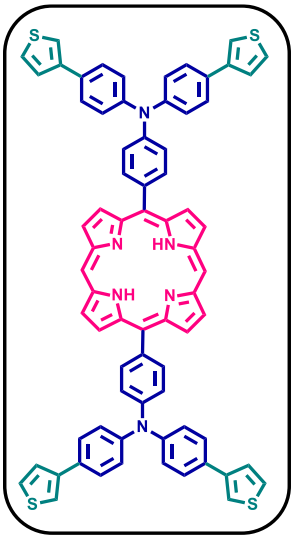


Purple powder. Yield: 22 %. $^{1}$H NMR (400 MHz, $CDCl_3$): δ (ppm) 10.321 (s, 2H), 9.428 (d, *J* = 4.4 Hz, 4H), 9.228 (d, *J* = 4.4 Hz, 4H), 8.157 (d, *J* = 8.4 Hz, 4H), 7.668 (d, *J* = 8.8 Hz, 4H), 7.549 (d, *J* = 8.4 Hz, 4H), 7.471-7.413 (m, 20H), 7.202-7.154 (m, 4H). $^{13}$C NMR ($CDCl_3$, 100 MHz): δ (ppm) 147.69, 147.39, 146.89, 145.06, 141.94, 135.90, 131.59, 131.03, 130.85, 129.61, 129.55, 127.51, 126.24, 125.08, 124.97, 124.87, 123.55, 121.84, 119.52, 118.97, 105.26.HRMS (ESI) m/z calcd for $C_{84}H_{52}F_{12}N_6$ $[M+H]^+$ 1125.289, found 1125.287.

**Compound 5b:**

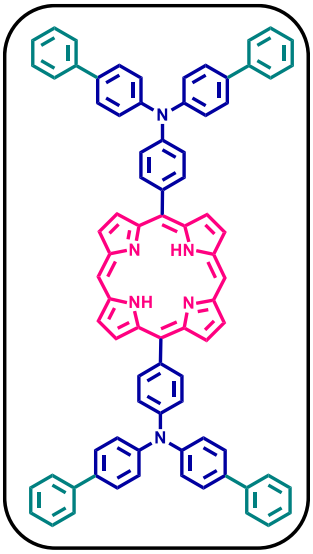

Purple powder. Yield: 30 %. $^{1}$H NMR (400 MHz, $CDCl_3$): δ (ppm) 10.326 (s, 2H), 9.435 (d, *J* = 3.6 Hz, 4H), 9.248 (d, *J* = 4 Hz, 4H), 8.191 (d, *J* = 7.6 Hz, 4H), 7.689 (d, *J* = 4 Hz, 16H), 7.619 (d, *J* = 7.6 Hz, 4H), 7.546 (d, *J* = 8 Hz, 8H), 7.492 (t, *J* = 7.2 Hz, 8H), 7.372 (t, *J* = 7.2 Hz, 4H), -3.003 (s, 2H). $^{13}$C NMR ($CDCl_3$, 100 MHz): δ (ppm) 147.39, 147.26, 147.00, 145.07, 140.65, 136.07, 135.96, 131.62, 131.03, 128.84, 128.18, 127.01, 126.81, 124.96, 122.16, 118.92, 105.29. (MALDI-TOF, m/z) calcd for $C_{80}H_{56}N_6$ $[M+H]^+$ 1101.463, found 1101.621.

**Compound 5c:**

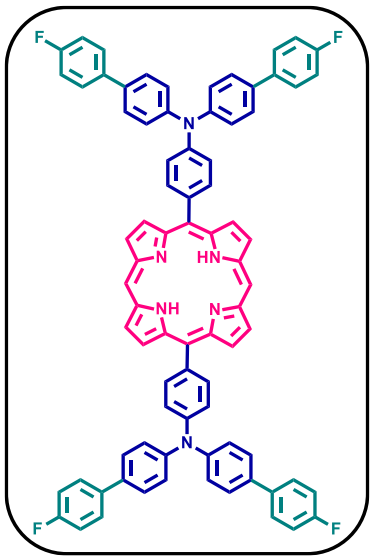

Purple powder. Yield: 22 %. $^{1}$H NMR (400 MHz, $CDCl_3$): δ (ppm) 10.336 (s, 2H), 9.443 (d, *J* = 3.6 Hz, 4H), 9.244 (d, *J* = 3.6 Hz, 4H), 8.195 (d, *J* = 8 Hz, 4H), 7.636 (m, *J* = 8.4 Hz, 20H), 7.531 (d, *J* = 8 Hz, 8H), 7.180 (t, *J* = 8.8 Hz, 8H), -3.009 (s, 2H). $^{13}$C NMR ($CDCl_3$, 100 MHz): δ (ppm) 162.45, 160.00, 146.31, 146.15, 145.87, 143.98, 135.72, 135.69, 134.93, 134.47, 134.06, 130.68, 130.01, 127.31, 127.23,

127.01, 123.97, 121.11, 117.84, 114.75, 114.54, 104.30. (MALDI-TOF, m/z) calcd for $C_{80}H_{52}F_4N_6$ $[M+H]^+$ 1173.426, found 1173.554.

**Compound 5d:**

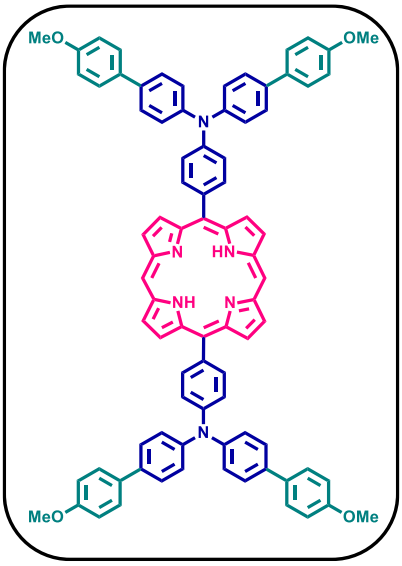


Purple powder. Yield: 46 %. $^1$H NMR (400 MHz, $CDCl_3$): δ (ppm) 10.323 (s, 2H), 9.434 (d, *J* = 4 Hz, 4H), 9.249 (d, *J* = 4 Hz, 4H), 8.176 (d, *J* = 8 Hz, 4H), 7.652-7.605 (m, 20H), 7.518 (d, *J* = 8 Hz, 8H), 7.019 (d, *J* = 8.4 Hz, 8H), 3.878 (s, 12H), -3.000 (s, 2H). $^{13}$C NMR ($CDCl_3$, 100 MHz): δ (ppm) 158.97, 147.45, 146.49, 145.07, 135.95, 135.79, 135.24, 133.28, 131.61, 131.06, 127.84, 127.73, 125.11, 121.84, 119.01, 114.29, 105.28, 55.39.MALDI-TOF, m/z calcd for $C_{84}H_{64}N_6O_4$ $[M+H]^+$ 1221.506, found 1221.682.

**Compound 5e:**

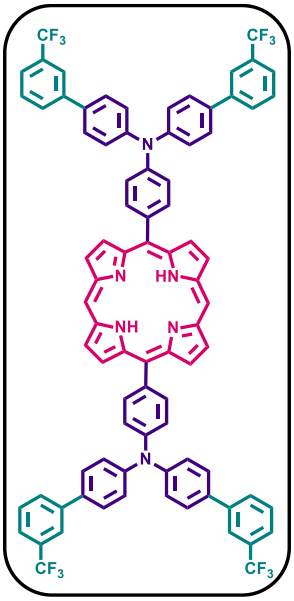


Purple powder. Yield: 18 %. $^{1}$H NMR (400 MHz, $CDCl_3$): δ (ppm) 10.351 (s, 2H), 9.457 (d, *J* = 4 Hz, 4H), 9.245 (d, *J* = 4 Hz, 4H), 8.226 (d, *J* = 8 Hz, 4H), 7.930 (s, 4H), 7.860 (d, *J* = 4.8 Hz, 4H), 7.708 (d, *J* = 7.6 Hz, 8H), 7.643-7.561 (m, 20H), -3.004 (s, 2H). $^{13}$C NMR ($CDCl_3$, 100 MHz): δ (ppm) 147.59, 146.95, 131.72, 131.00, 130.02, 129.33, 128.35, 124.92, 123.62, 122.90, 118.75, 105.38. (MALDI-TOF, m/z) calcd for $C_{84}H_{52}F_{12}N_6$ $[M+H]^+$ 1373.413, found 1373.606.

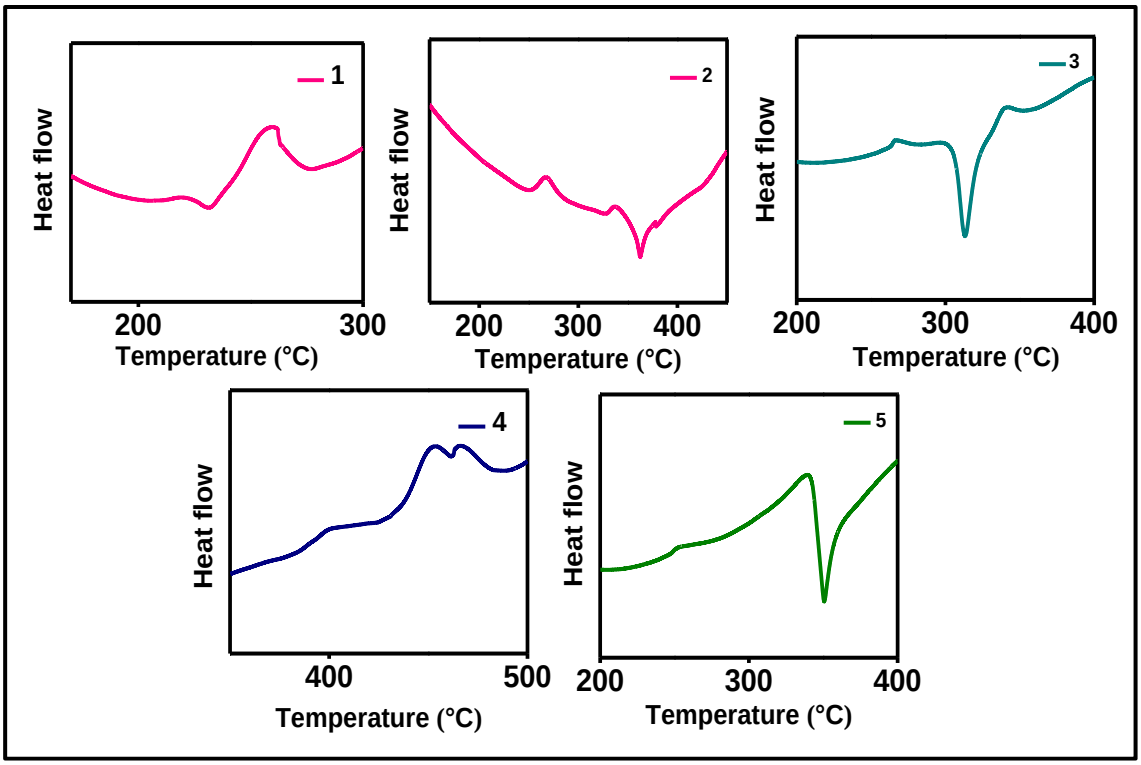


**Figure S1**. DSC Thermogram of compounds **5a-e**.

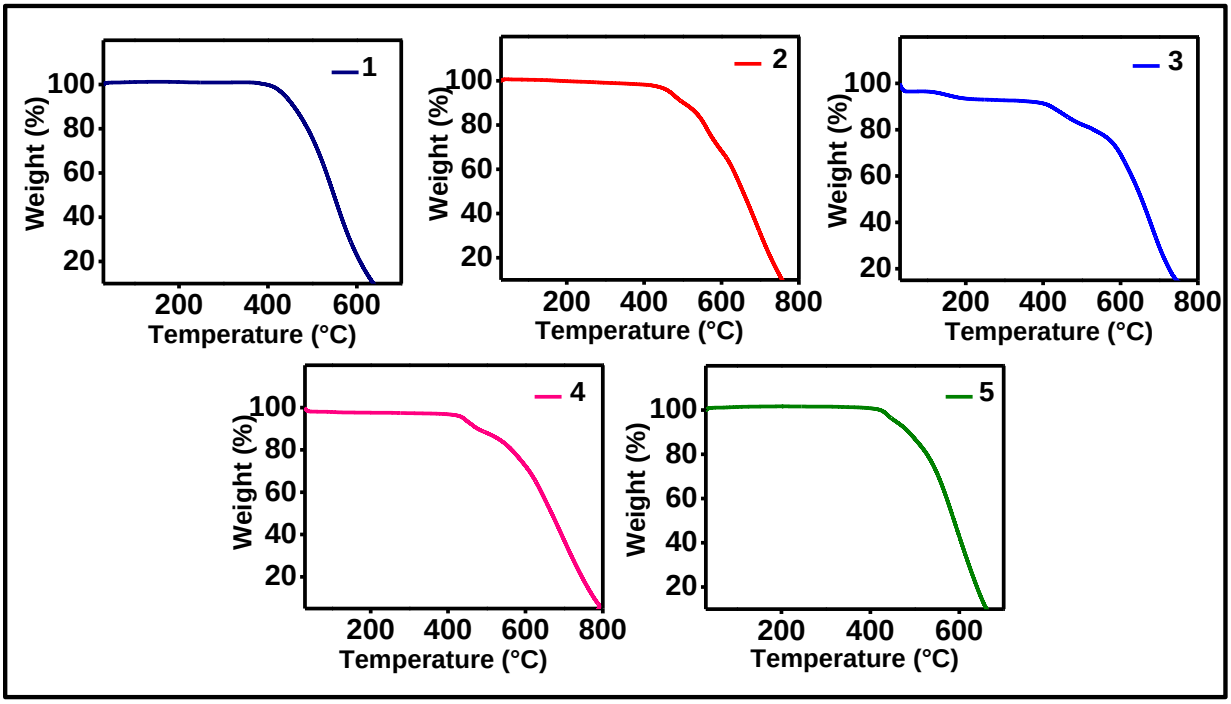


**Figure S2**. TGA Thermogram of compounds **5a-e**.

**Table S1**. Melting point and decomposition temperature for 10 % weight loss of compounds

| C. No. | $T_m$(°C) | $T_d$(°C) |
|---|---|---|
| **5a** | 396 | 461 |
| **5b** | 363 | 504 |
| **5c** | 313 | 422 |
| **5d** | 461 | 479 |
| **5e** | 351 | 489 |

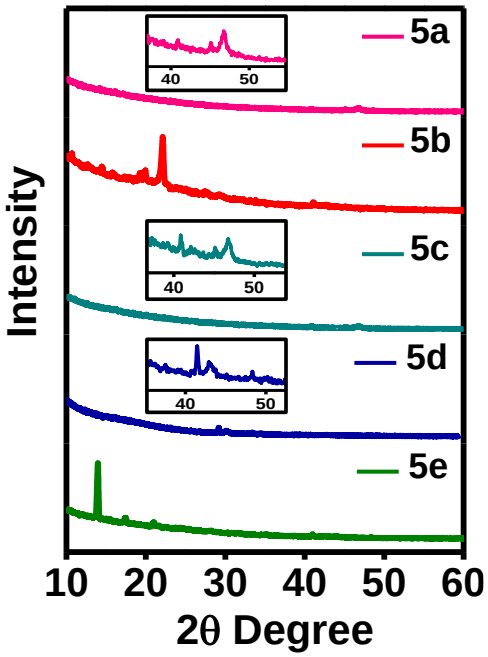


**Figure S3**. GIXRD of compounds **5a-e**

## Computational studies:

DFT and TD-DFT calculations were carried out for compounds **5a-e** to gain an insight into their electronic structures. Porphyrin molecules with different TAA were explored theoretically to observe their electronic and charge transport properties. DFT: B3LYP *ab initio* approach was employed to elucidate the structural properties of all molecules. The optimization of all compounds were done starting from MOPAC and ending with Gaussian at the DFT-B3LYP (6-31g*) level of theory for ground state

(S0).From the TD-DFT calculations, the oscillator strength value (F) obtained demonstrated all the compounds have $S_0$-$S_1$,$S_3$- $T_1$ and $S_3$-$T_2$ transitions.The reorganization energies i.e., energy relaxation during transport was obtained from the changes in bond length acquired from a few important centers.To clarify the impact of substituent on the optical properties substituted porphyrins, the electronic transitions at the optimized structures also have been calculated by time-dependent DFT (TD-DFT) calculations. The maximum absorption wavelengths, oscillator strength (f) and corresponding transition assignment are listed in **Table S2.** The geometrical parameters suggested that all compounds in which substituted TAA groups were exhibited non-planar whereas porphyrin core moiety obtained as planar. From medeA data, the carrier mobilities of all thecompounds revealedin the range of $10^{-6}$ $m^2$ $V^{-1}s^{-1}$. The values are given in the **TableS2**. Compound **5e** achieved up to the value of $8.6046x10^{-6}$, the highest among the series. It might be due to the presence of electron withdrawing group.

**Table S2**. Electronic absorption behavior of compounds **5a-e** by TD-DFT.

| C. No. | Electronic Transition | Wavelength nm | Energy eV | Oscillator strength (f) | Type of transition | Hole Transport ($m^2$/Vs) 300K |
|---|---|---|---|---|---|---|
| **5a** | Ex3=290-295 | 604.16 | 2.052 (16550$cm^{-1}$) | 0.000 | $S_{-3}$-$T_2$ | $2.8099x10^{-6}$ |
| **5b** | Ex3=286-290 | 623.5 | 1.988 (160343$cm^{-1}$) | 0.000 | $S_{-3}$-$T_1$ | $6.7825x10^{-6}$ |
| **5c** | Ex3=302-307 | 603.0 | 2.056 (16582$cm^{-1}$) | 0.000 | $S_{-3}$-$T_2$ | $5.7527x10^{-6}$ |
| **5d** | Ex3=353-354 | 608.5 | 2.037 (16429$cm^{-1}$) | 0.513 (52%) | $S_0$-$S_1$ | $8.6046x10^{-6}$ |
| **5e** | Ex3=321-322 | 619.1 | 2.002 (16147$cm^{-1}$) | 0.581 (67%) | $S_0$-$S_1$ | $3.2984x10^{-6}$ |

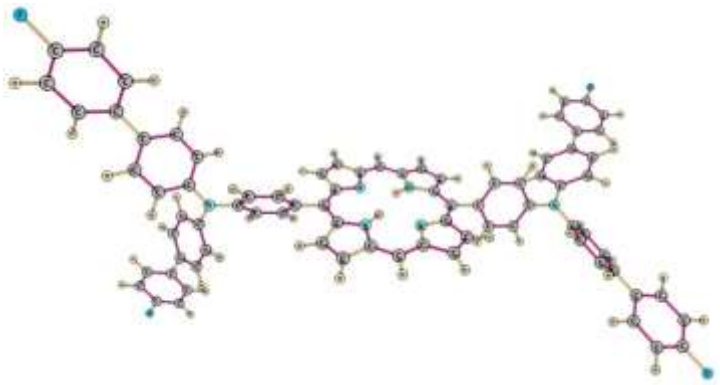

**Figure S4**. Generalized representation of the molecule

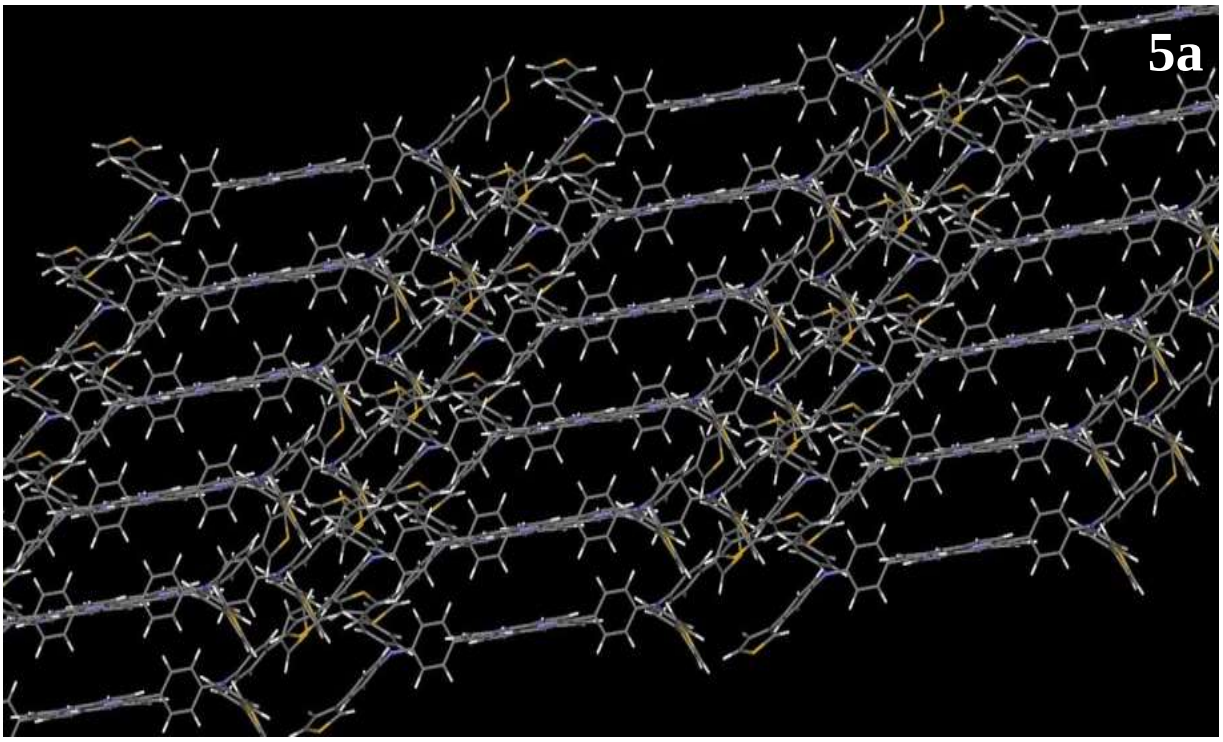
5a

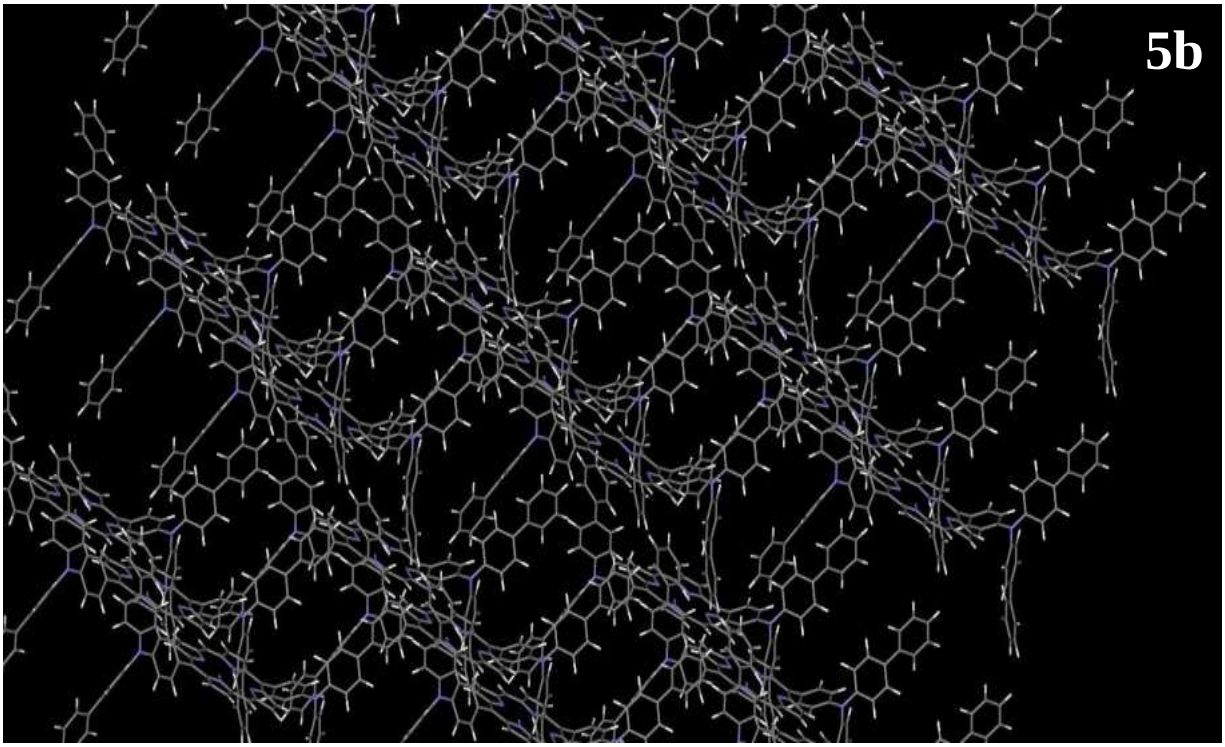
5b

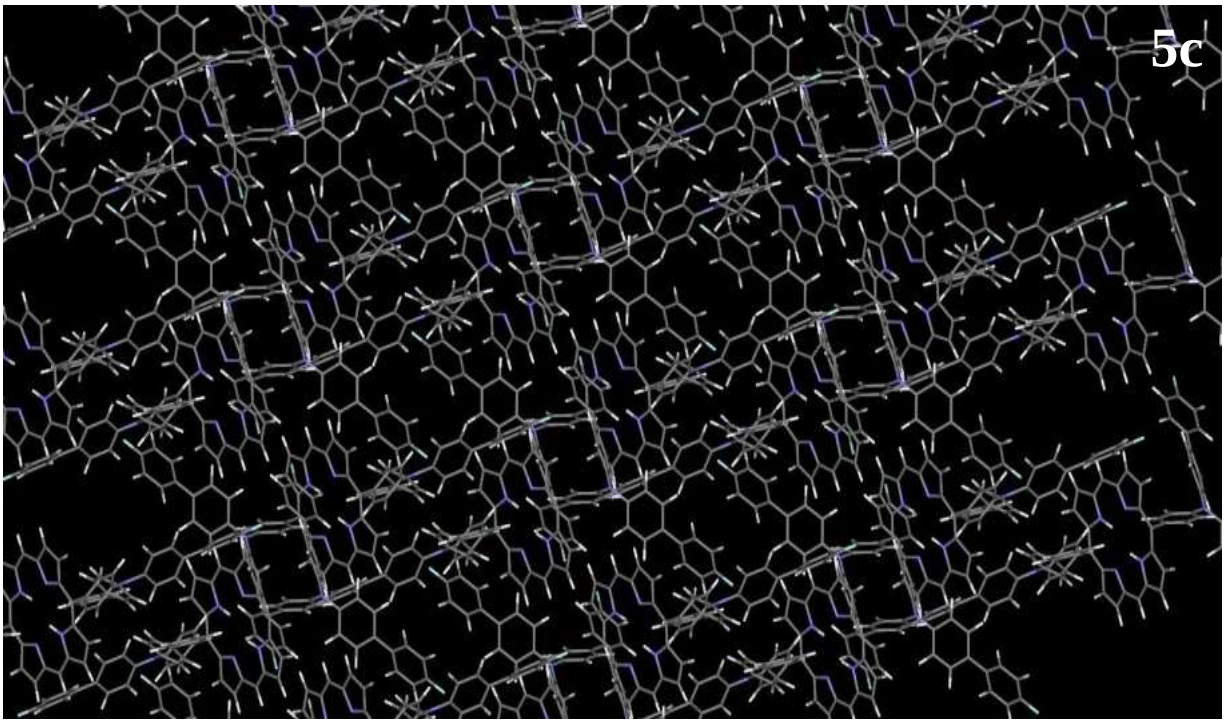
5c

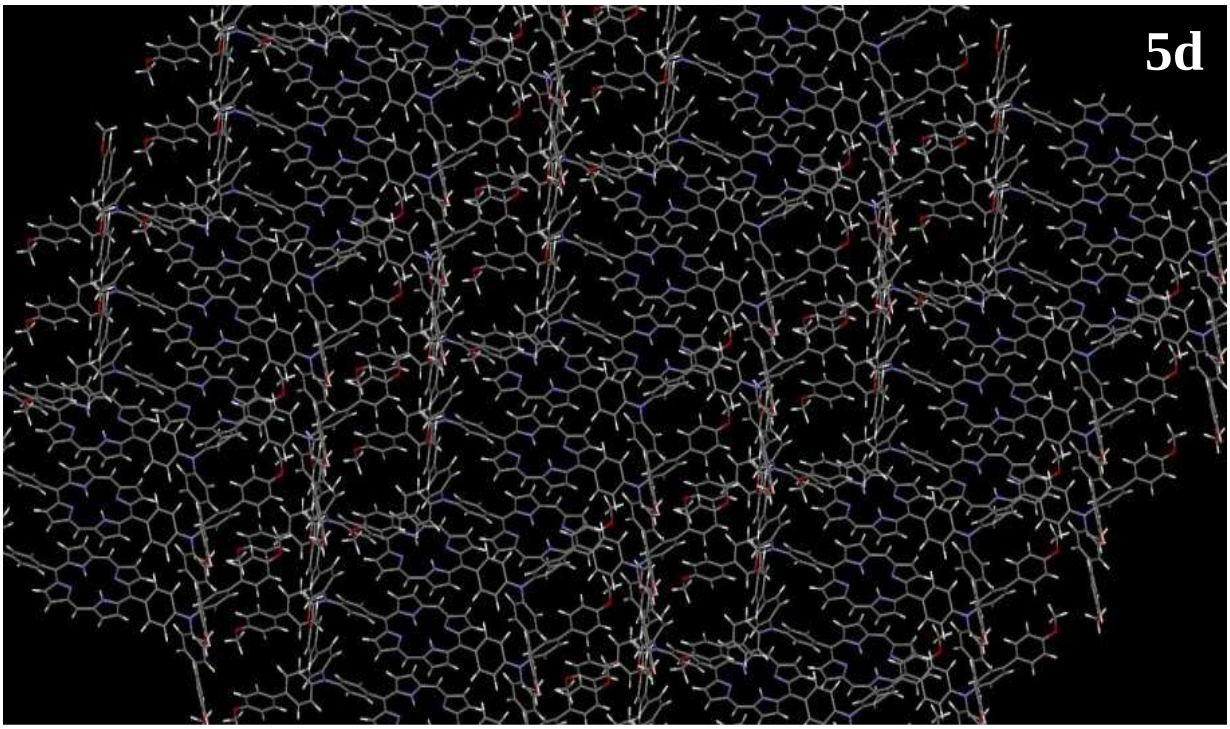
5d

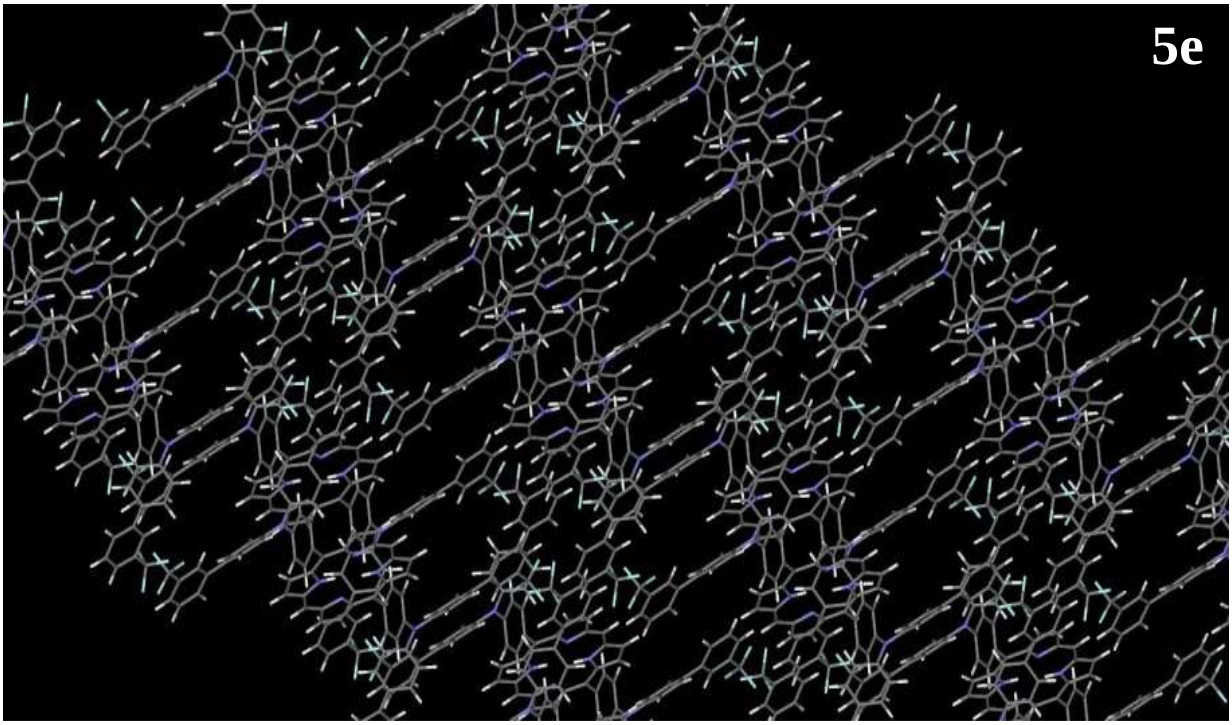


**Figure S5.** Molecular packing of compounds **5a-e**.

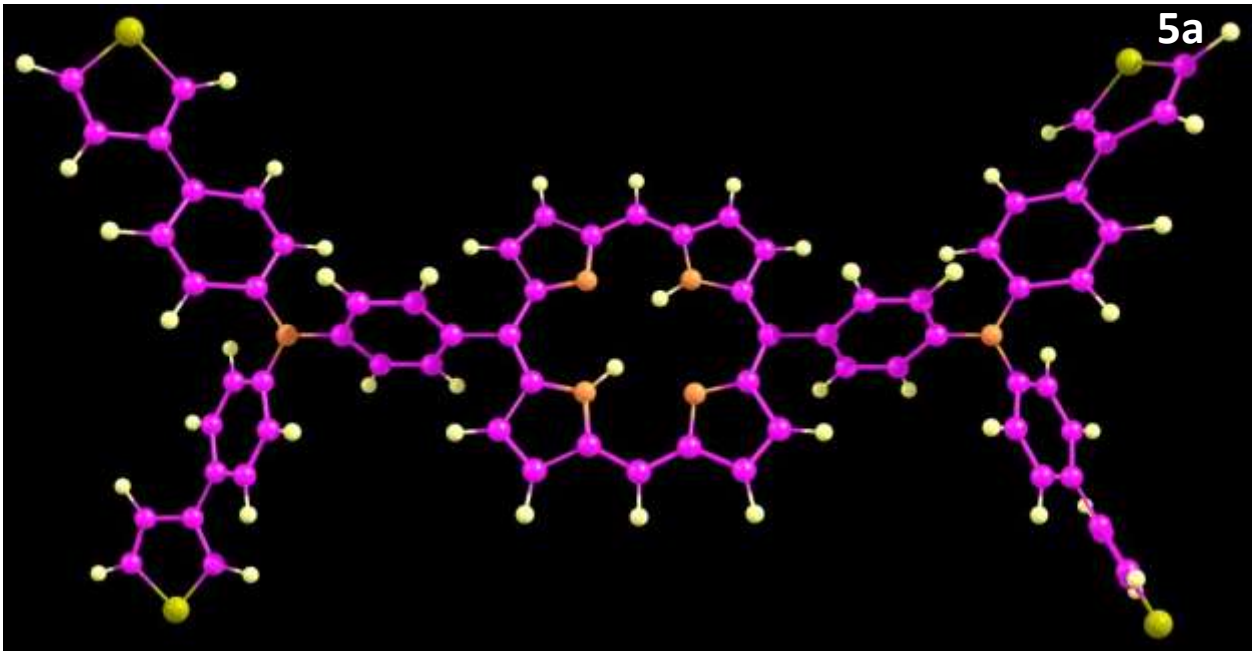

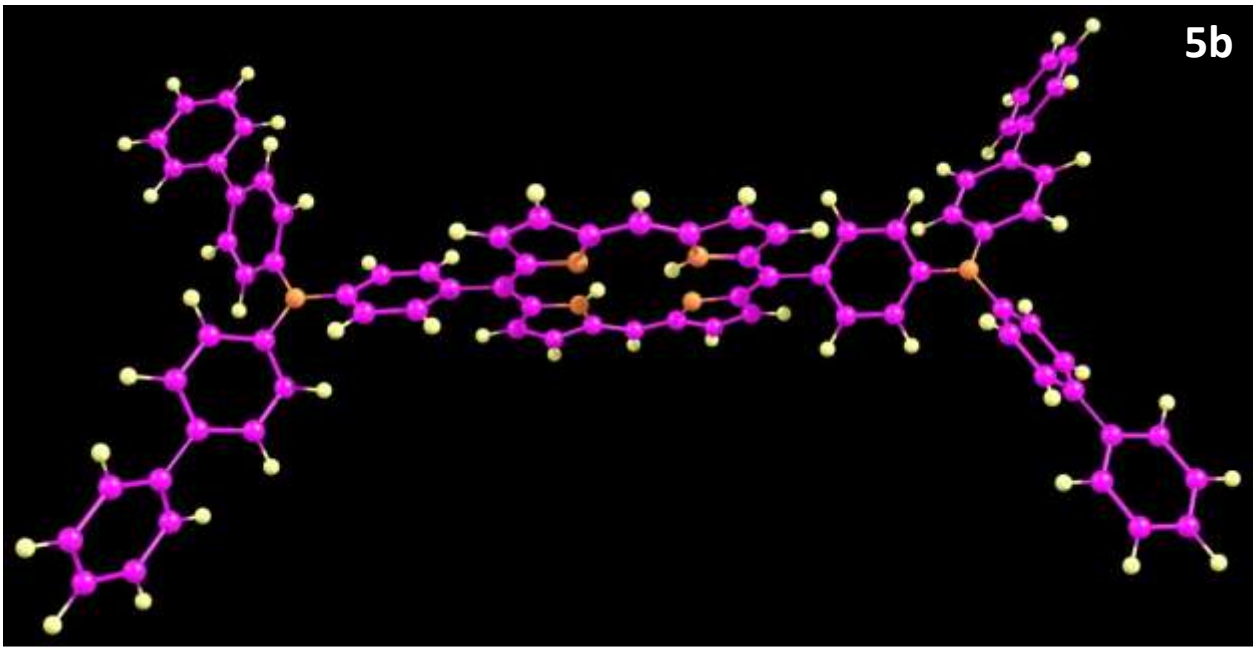
5b

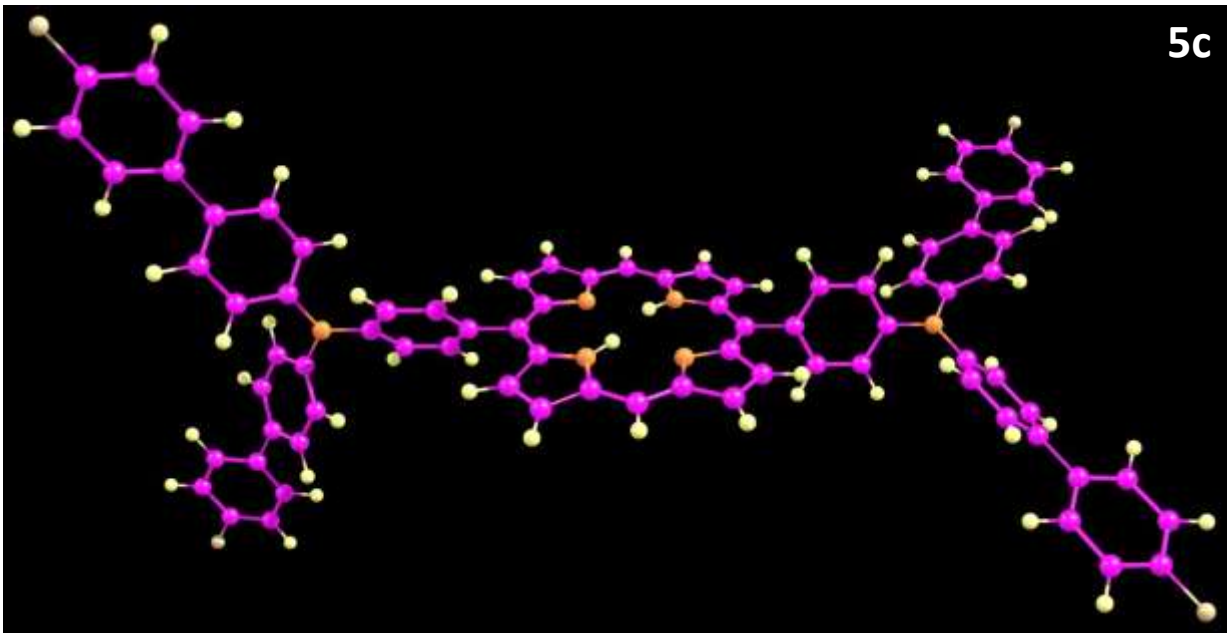
5c

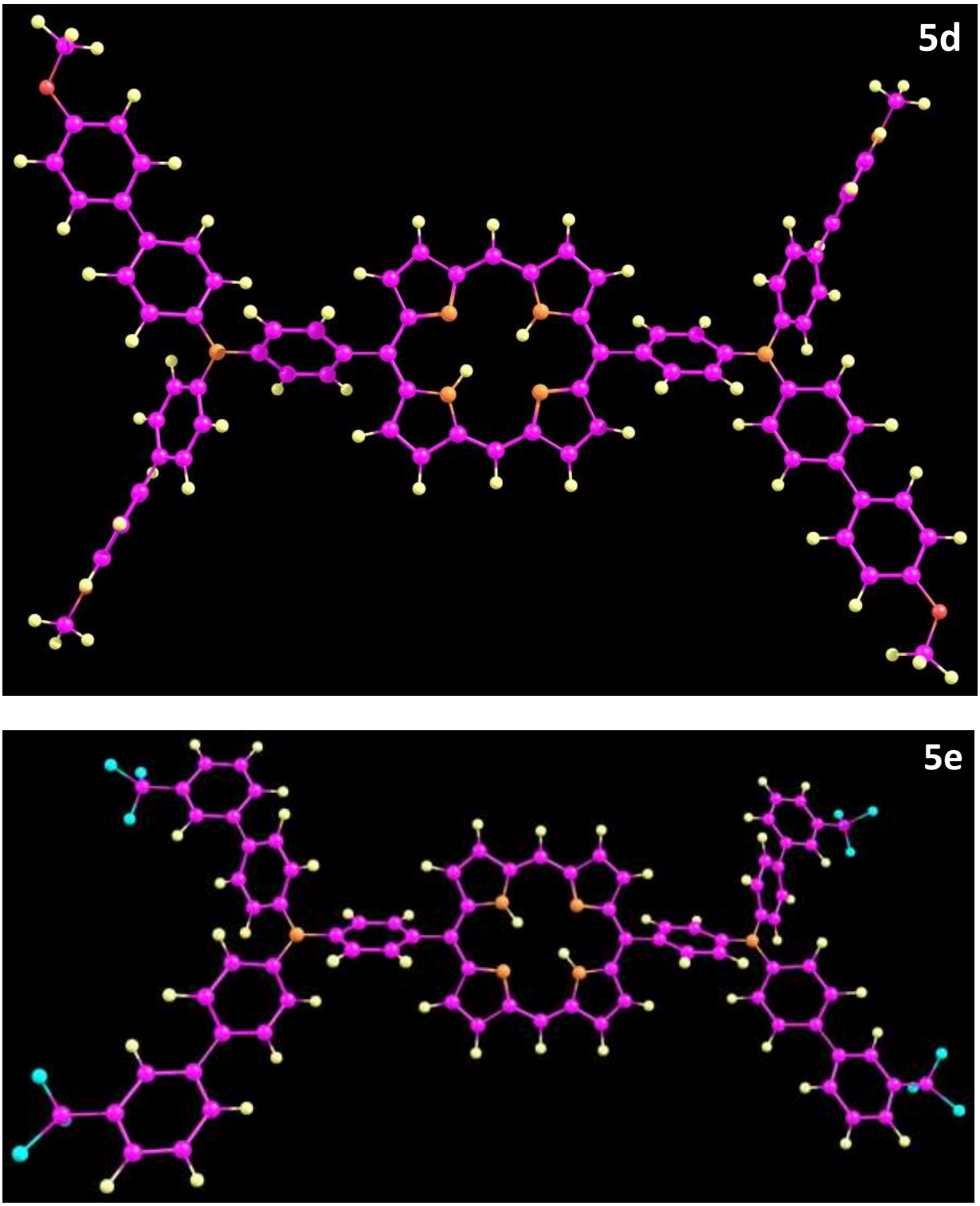


**Figure S6.**Optimized geometry of compounds **5a-e**.

**Table S3**. Grain size of compounds **5a-e**

| C. No. | Grain size(µm) |
|---|---|
| **5a** | 1.83 |
| **5b** | 0.51 |
| **5c** | 5.13 |
| **5d** | 3.02 |
| **5e** | 8.10 |

**Table S4**. d-spacing of compounds **5a-e**

| C. No. | d-spacing(nm) |
|---|---|
| **5a** | 1.944 |
| **5b** | 4.041 |
| **5c** | 1.946 |
| **5d** | 2.178 |
| **5e** | 6.363 |

**Device fabrication**

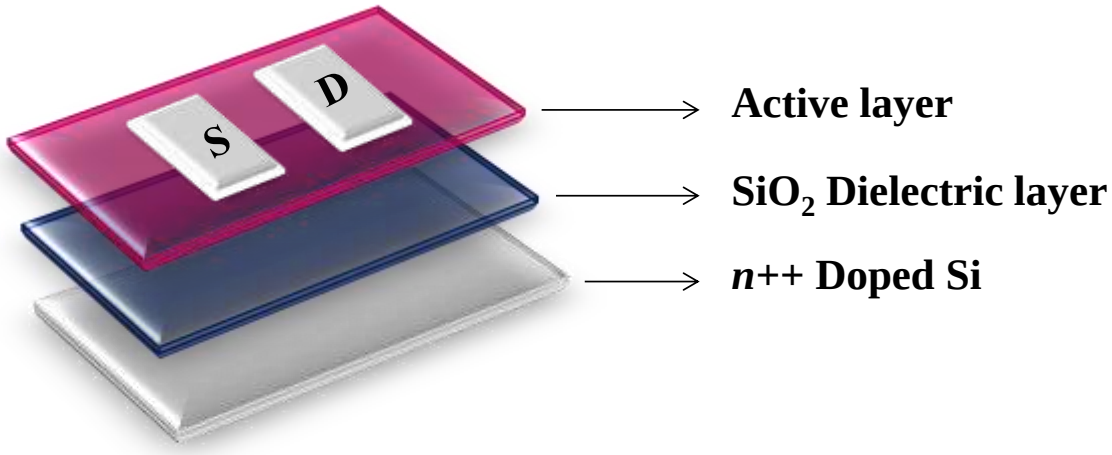


**Figure S7.** Schematic representation of the OFET device

Field-effect mobility of porphyrins was measured by employing bottom gate top contact architecture for device fabrication represented as in the Figure S6. The heavily doped $n^{++}$ Si substrate treated as the gate electrode and thermally grown $SiO_2$ (300 nm) acts as a gate

dielectric. Active semiconducting material coated over $SiO_2$ by spin coating method using chloroform and annealed at 100 °C for one hour to obtain uniform film and also to remove the residual solvents. Silver electrodes were made over active layer as source and drain electrode with a channel length of 150 μm and a width of 5 mm was used and again annealed as earlier. The fabricated device showed *p*-type behavior for all the compounds.

**Reliability factor and effective mobility calculation**

The reliability factor was calculated for all the compounds which define the ratio of the maximum channel conductivity experimentally achieved in a FET at the maximum gate voltage to the maximum channel conductivity expected in a correctly functioning ideal FET. In the saturation regime, the reliability factor is calculated using the equation 1.

$$r_{sat} = \left(\frac{\sqrt{|I_{SD}|^{max}} - \sqrt{|I_{SD}|^{0}}}{|V_{GS}|^{max}}\right)^2 \Big/ \left(\frac{WC_i}{2L}\mu_{sat}\right)_{claimed}$$

$$= \left(\frac{\sqrt{|I_{SD}|^{max}} - \sqrt{|I_{SD}|^{0}}}{|V_{GS}|^{max}}\right)^2 \Big/ \left(\frac{\partial\sqrt{|I_{SD}|}}{|V_{GS}|}\right)^2_{claimed} \qquad (1)$$

whereas, $\mu_{sat}$ is the calculated mobility, L, W and $C_i$ are the device parameters, and $|I_{SD}|^{max}$ denotes the experimental maximum source–drain current reached at the maximum gate voltage $|V_{GS}|^{max}$ and $|I_{SD}|^{0}$ represents the source–drain current at $V_{GS}$= 0.

By using the calculated reliability factor and claim mobility the effective mobility is measured from equation 2.

$$\mu_{eff} = r \times \mu_{claimed} \qquad (2)$$

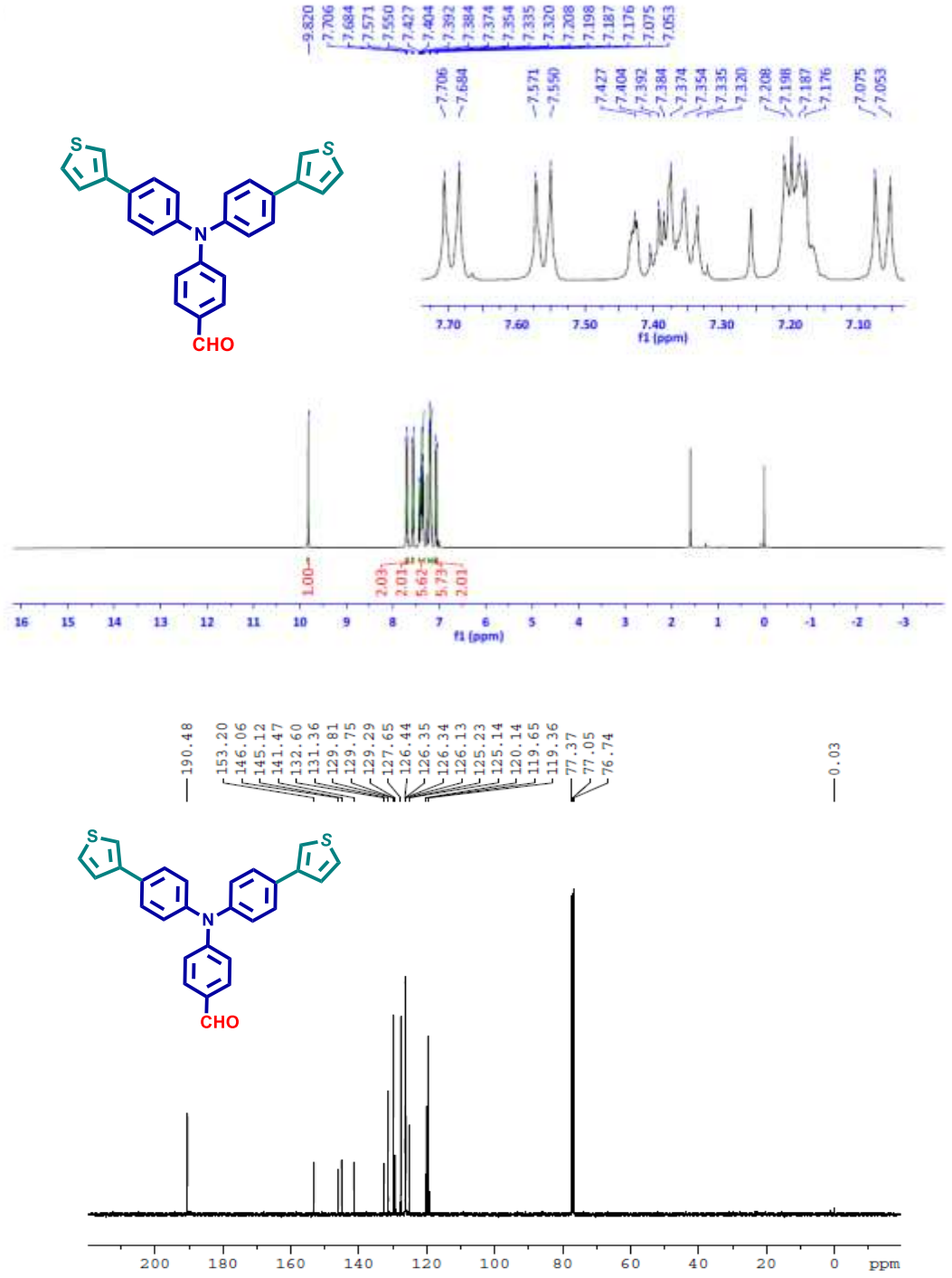


**Figure S8.** $^{1}$H NMR and $^{13}$C NMR spectra of compound **3a**.

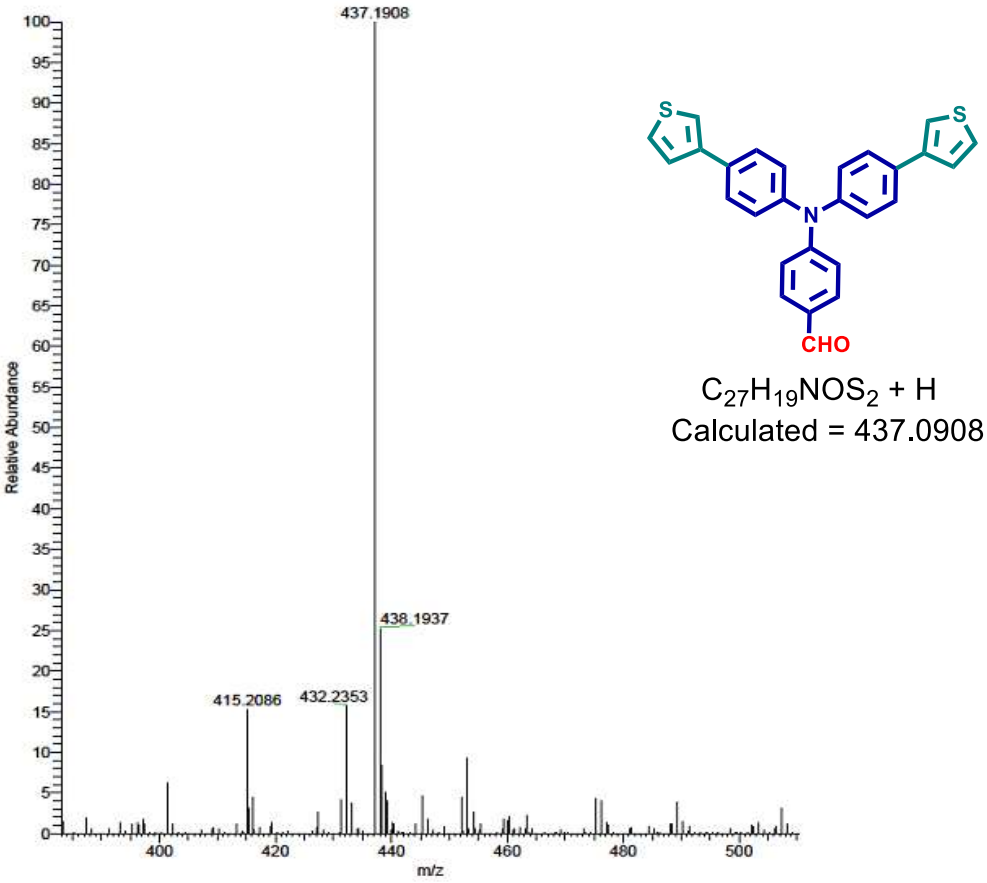


**Figure S9.** HR-Mass spectrum of **3a**.

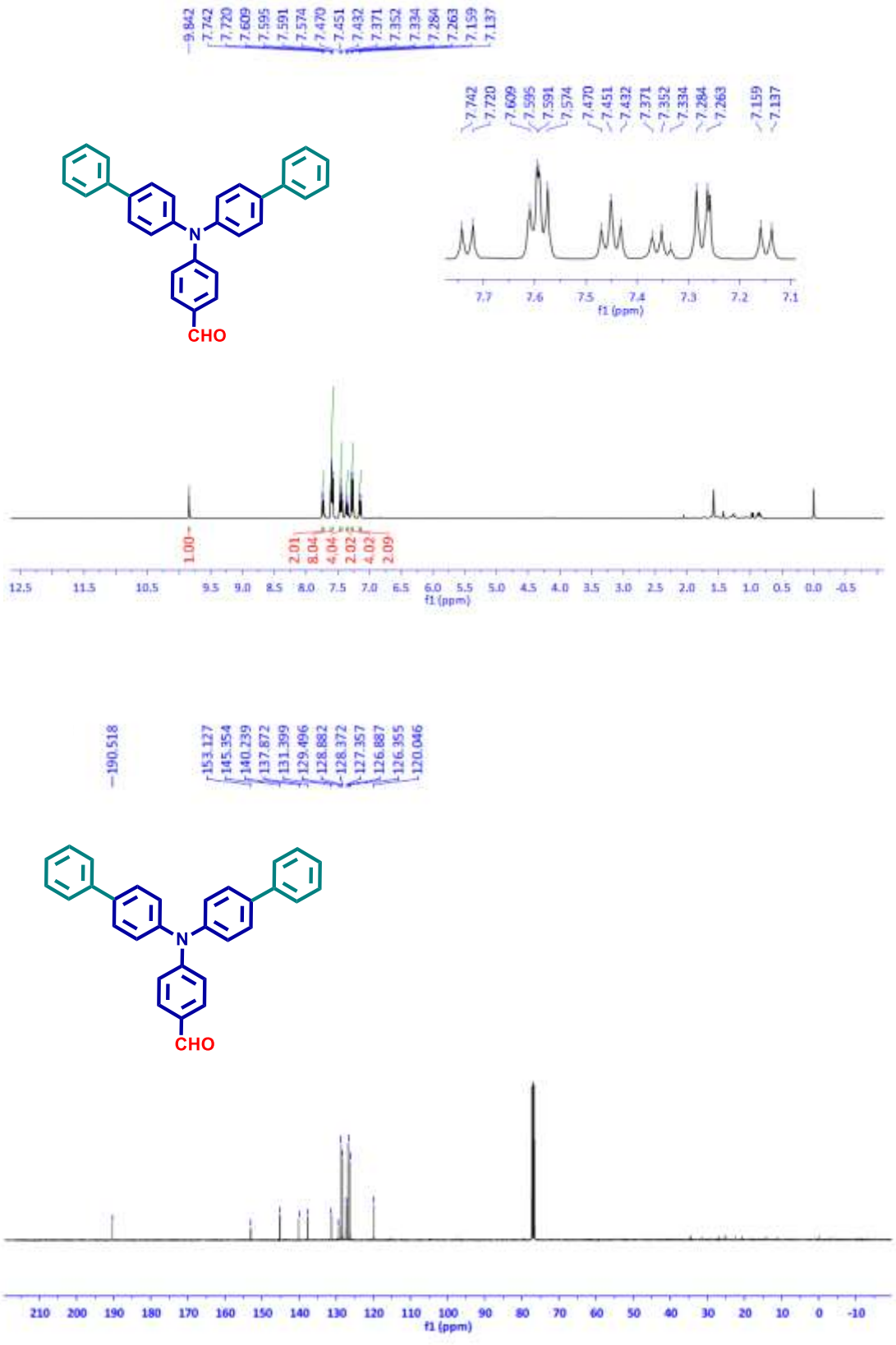


**Figure S10.**[1]H NMR and [13]C NMR spectra of **3b**.

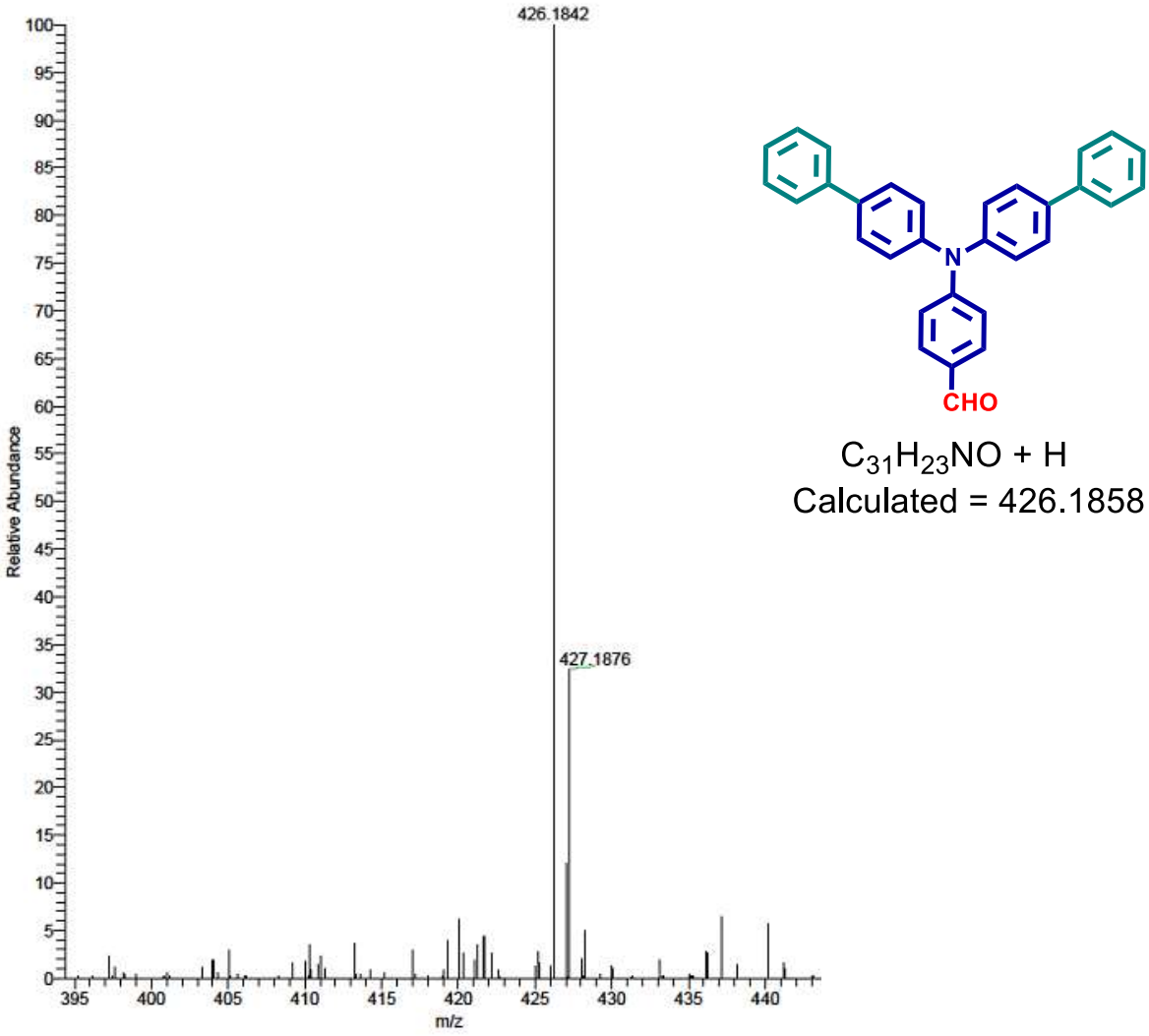


**Figure S11.** HR-MS spectrum of **3b**.

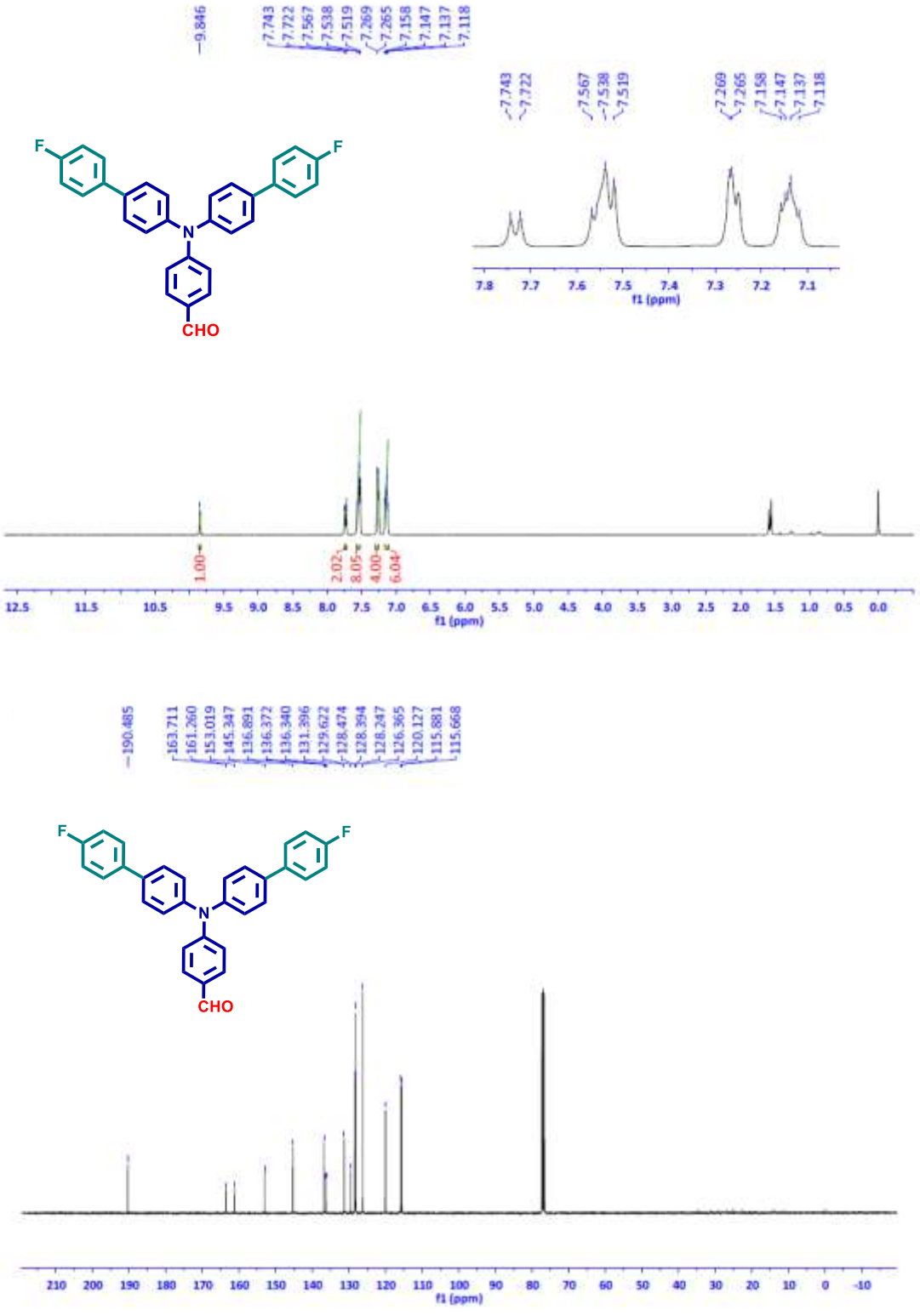


**Figure S12.** $^{1}$H NMR and $^{13}$C NMR spectra of **3c**.

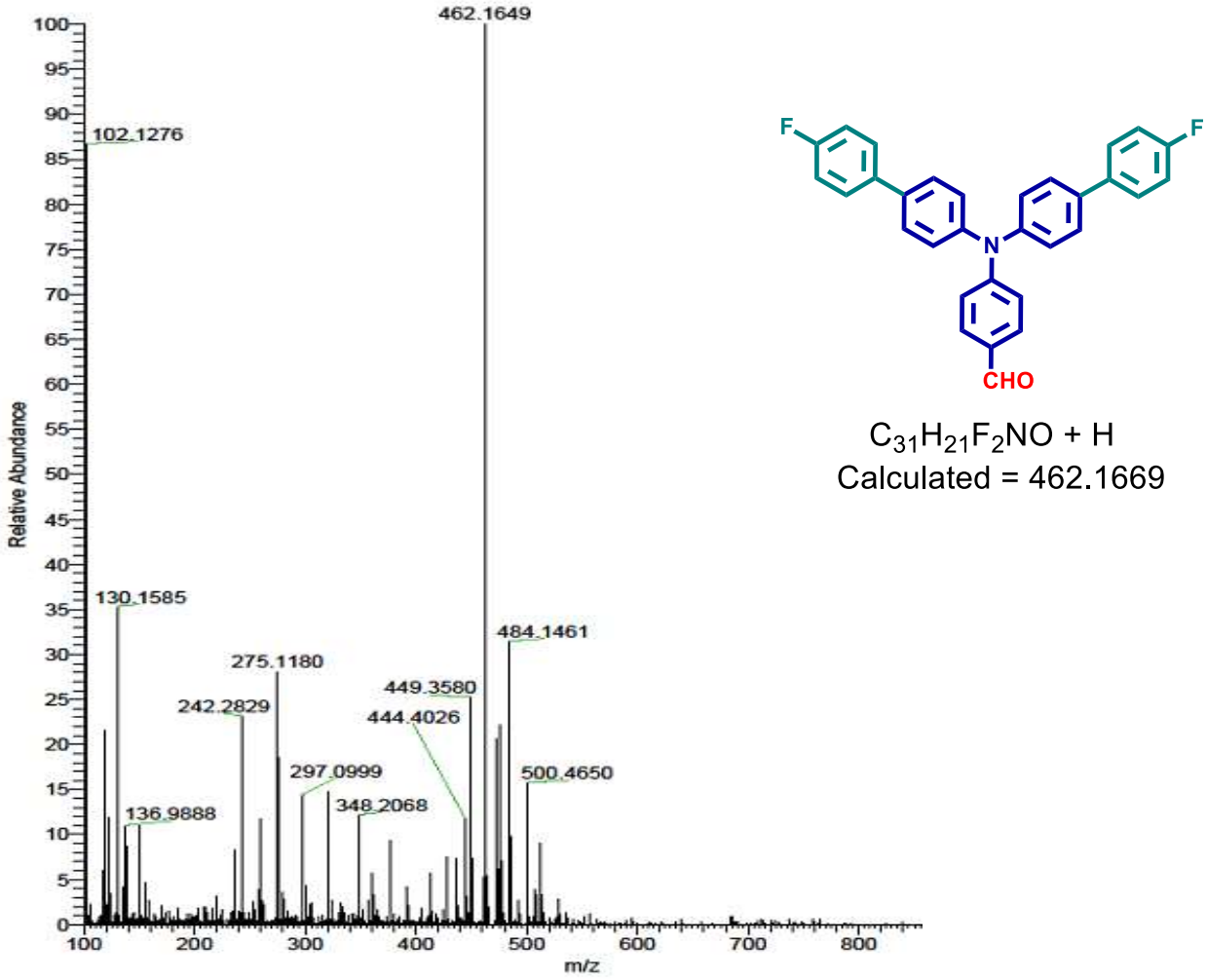


**Figure S13.** HR-Mass spectrum of **3c**.

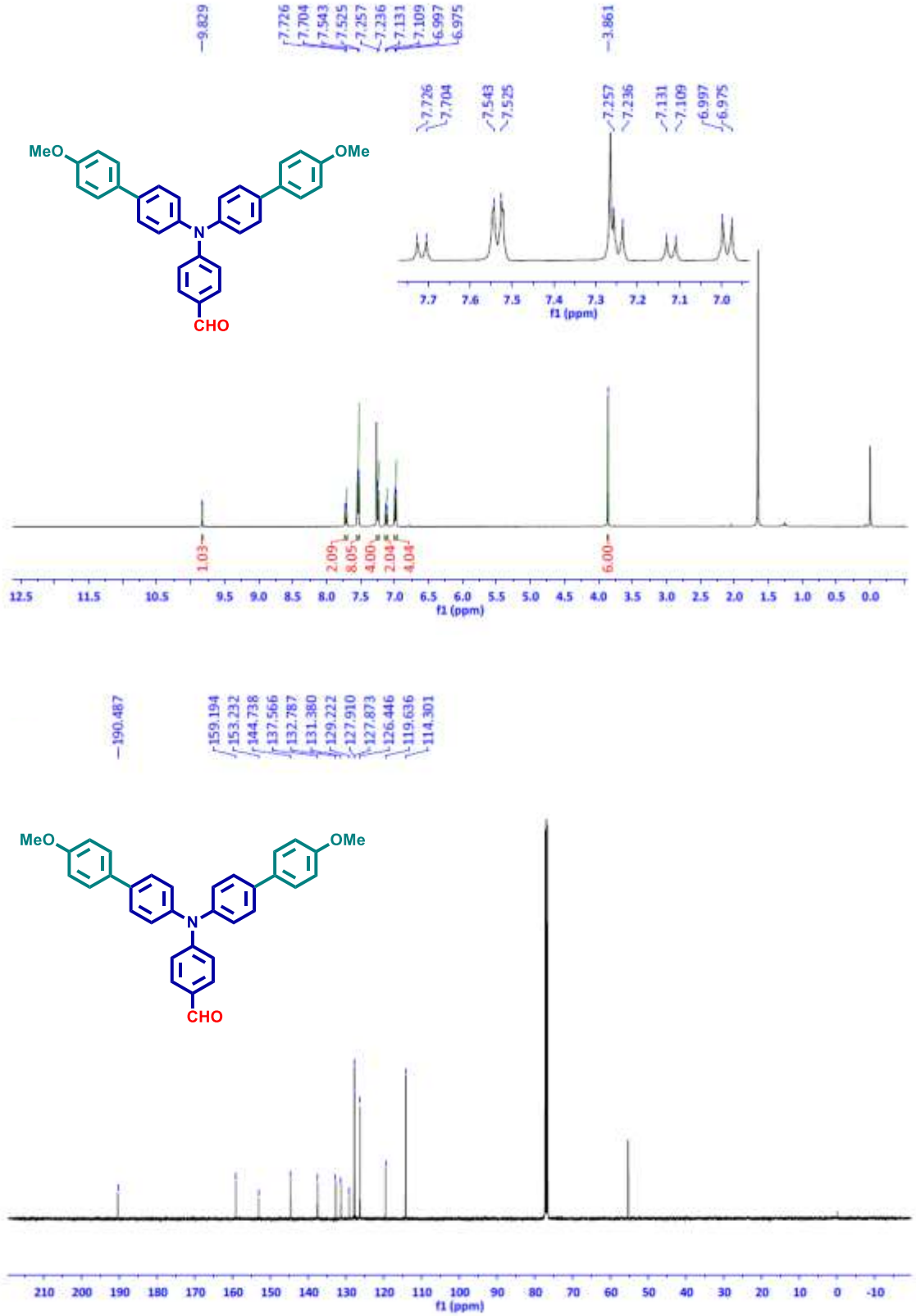


**Figure S14.** $^{1}$H NMR and $^{13}$C NMR spectra of **3d**.

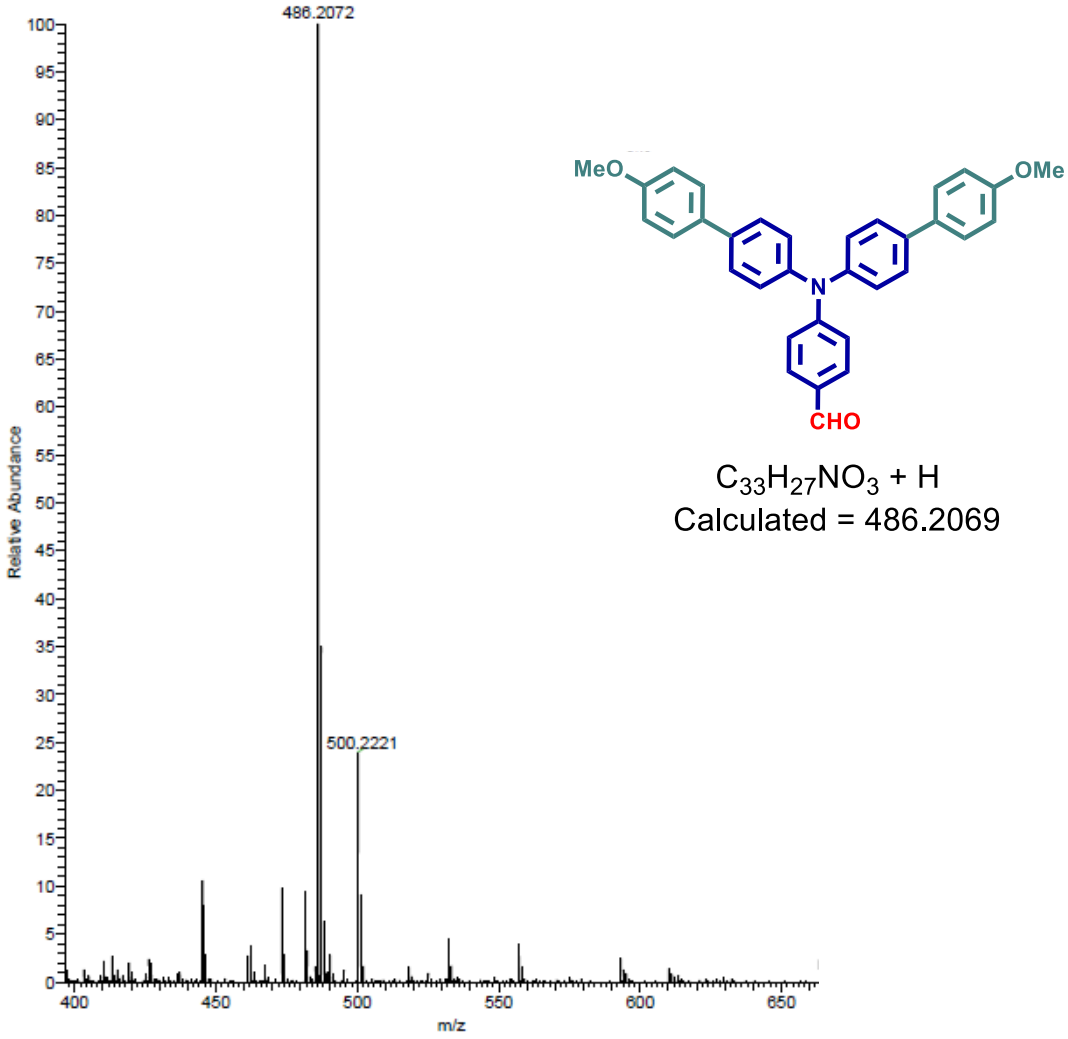


**Figure S15.** HR-Mass spectrum of **3d**.

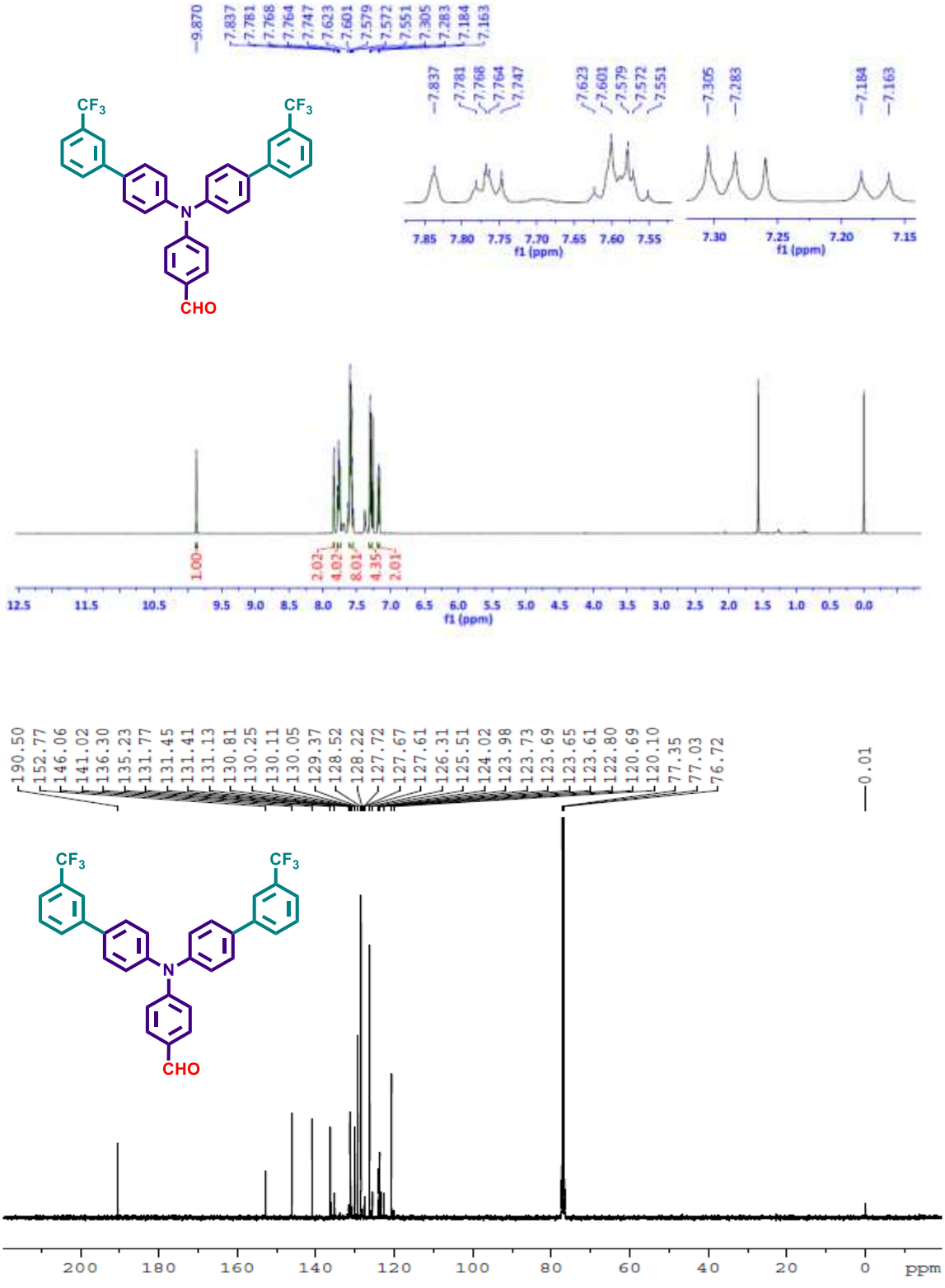


**Figure S16.** $^{1}$H NMR and $^{13}$C NMR spectra of **3e**.

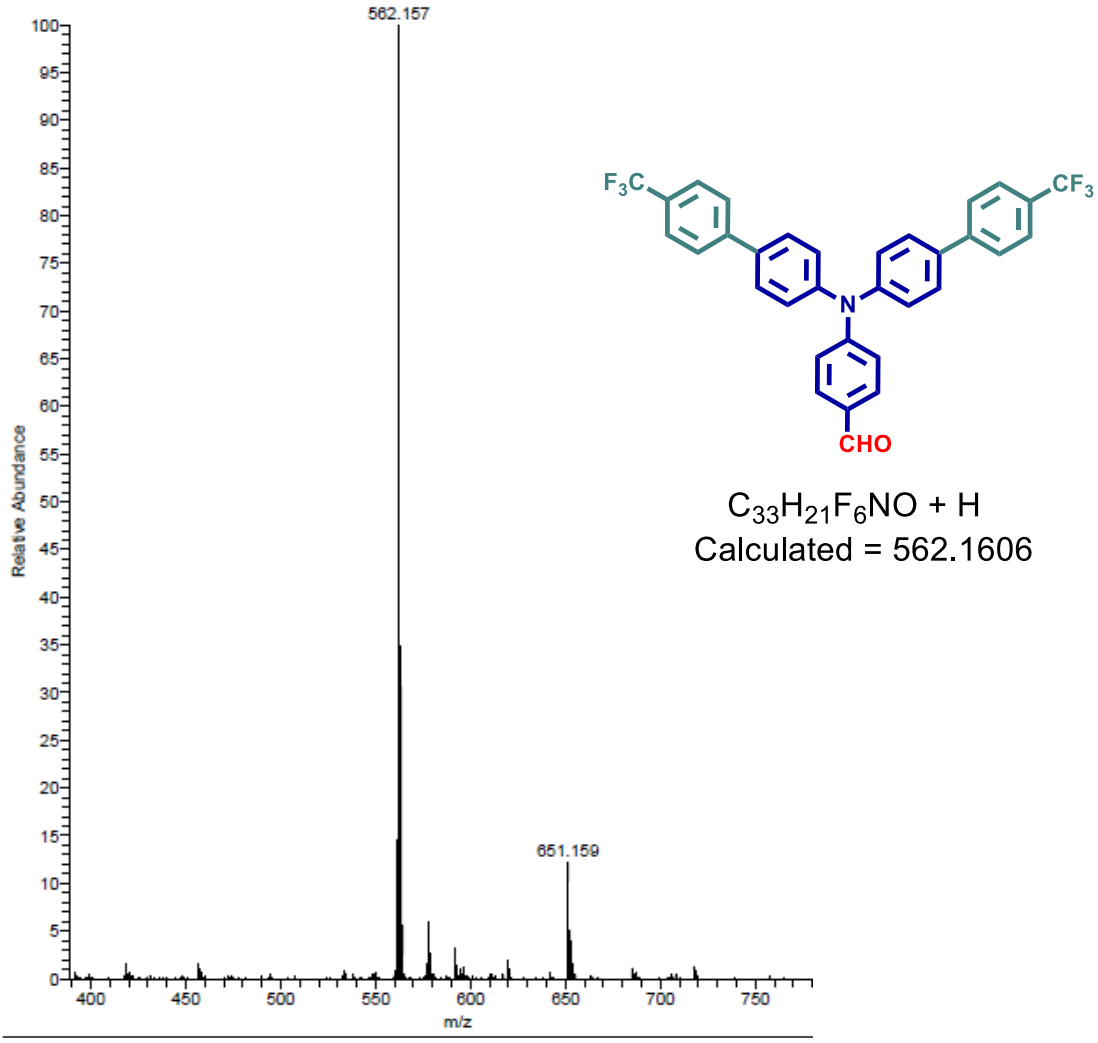


**Figure S17.** HR-Mass spectrum of **3e**.

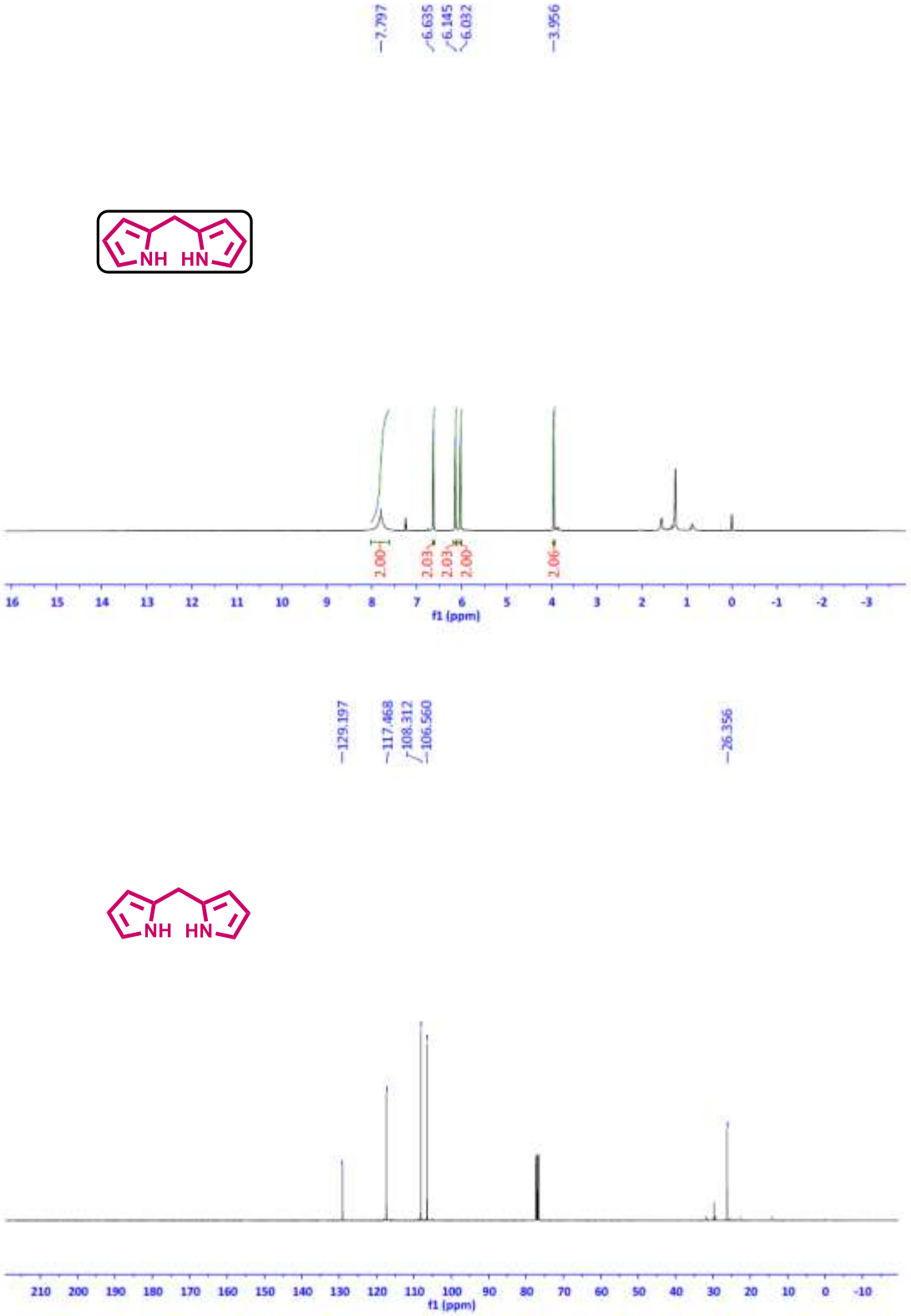


**Figure S18.** $^{1}$H NMR and $^{13}$C NMR spectra of **4**.

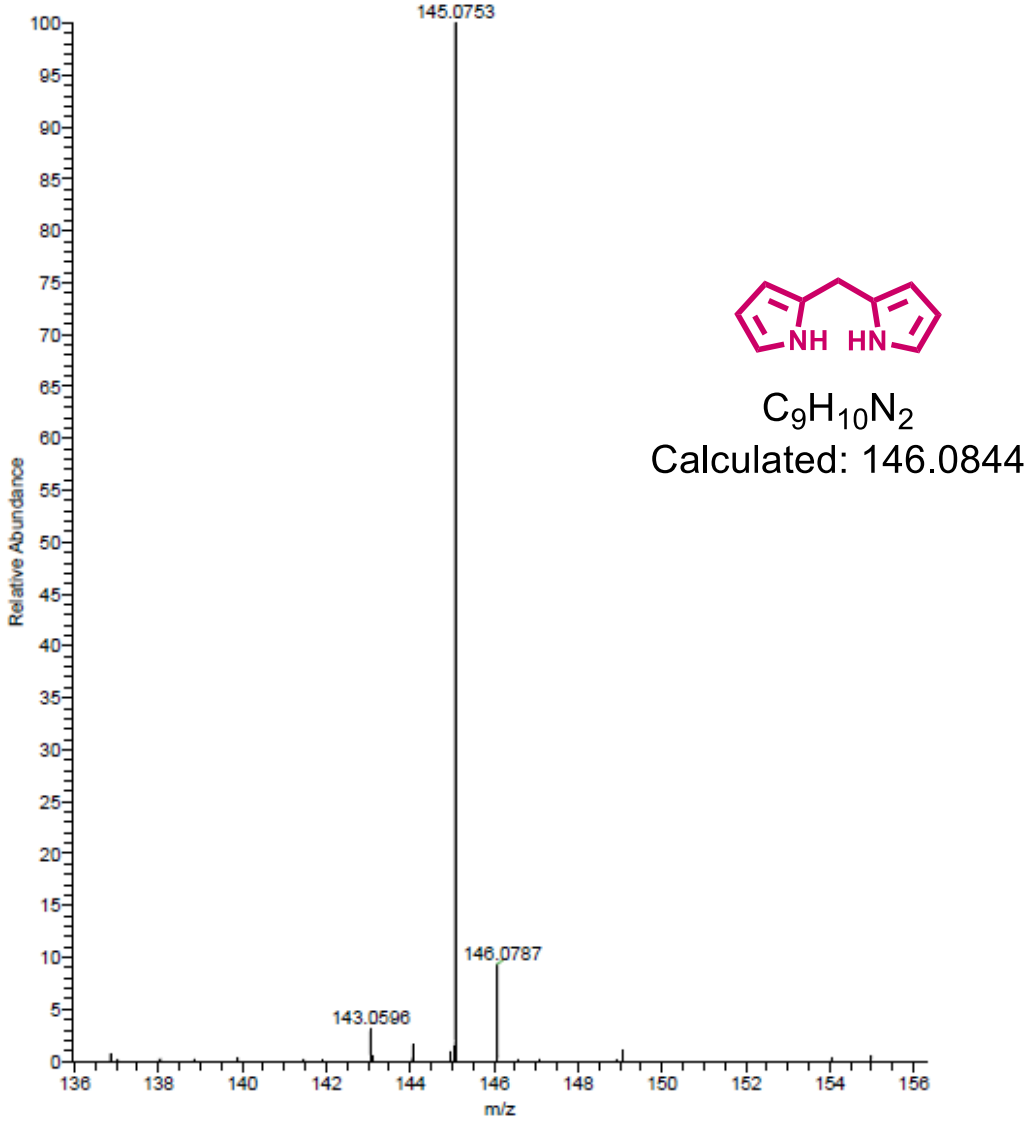


**Figure S19.** HR-Mass spectrum of compound **4**.

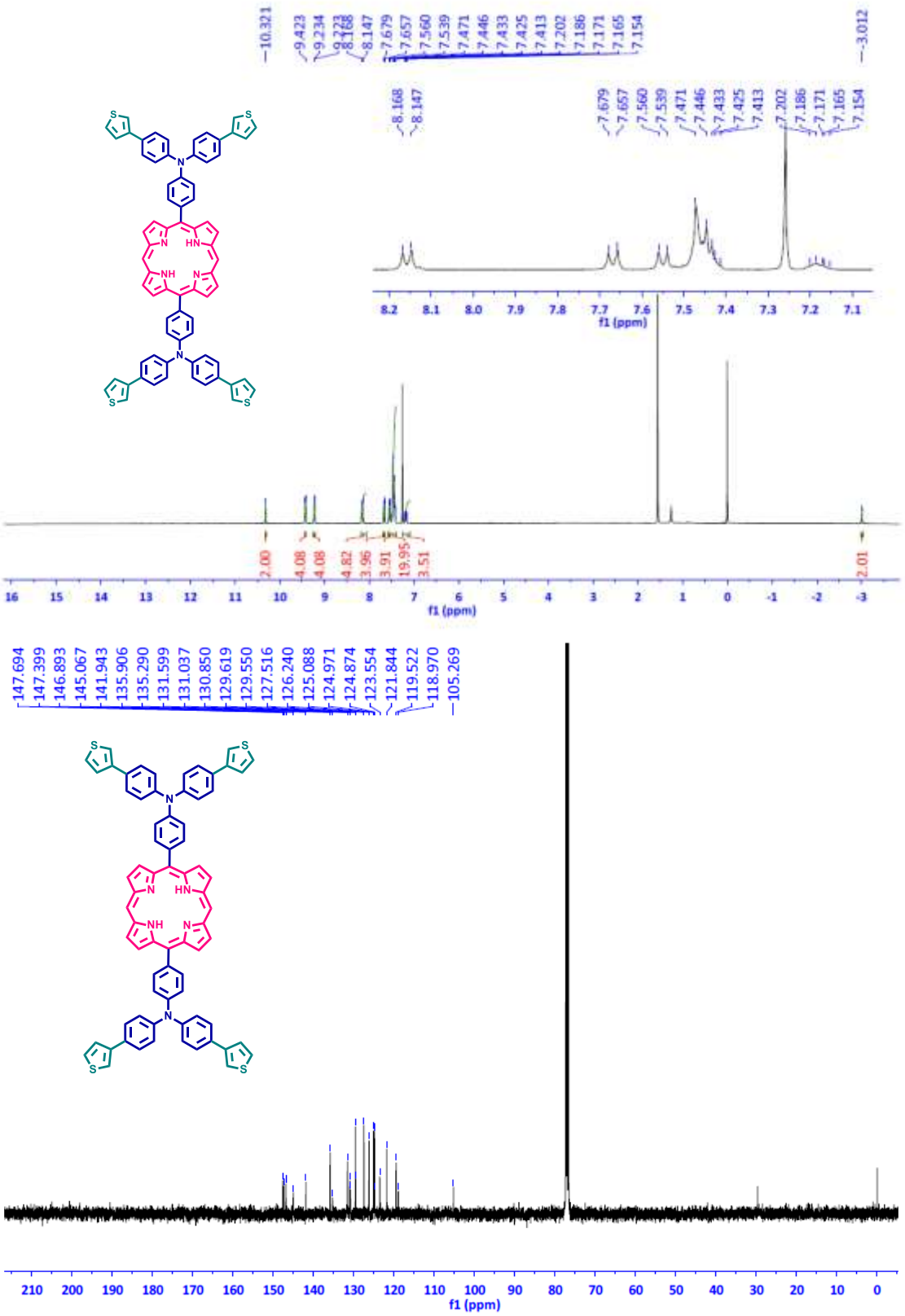


**Figure S20.**[1]H NMR and [13]C NMR spectra of **5a**.

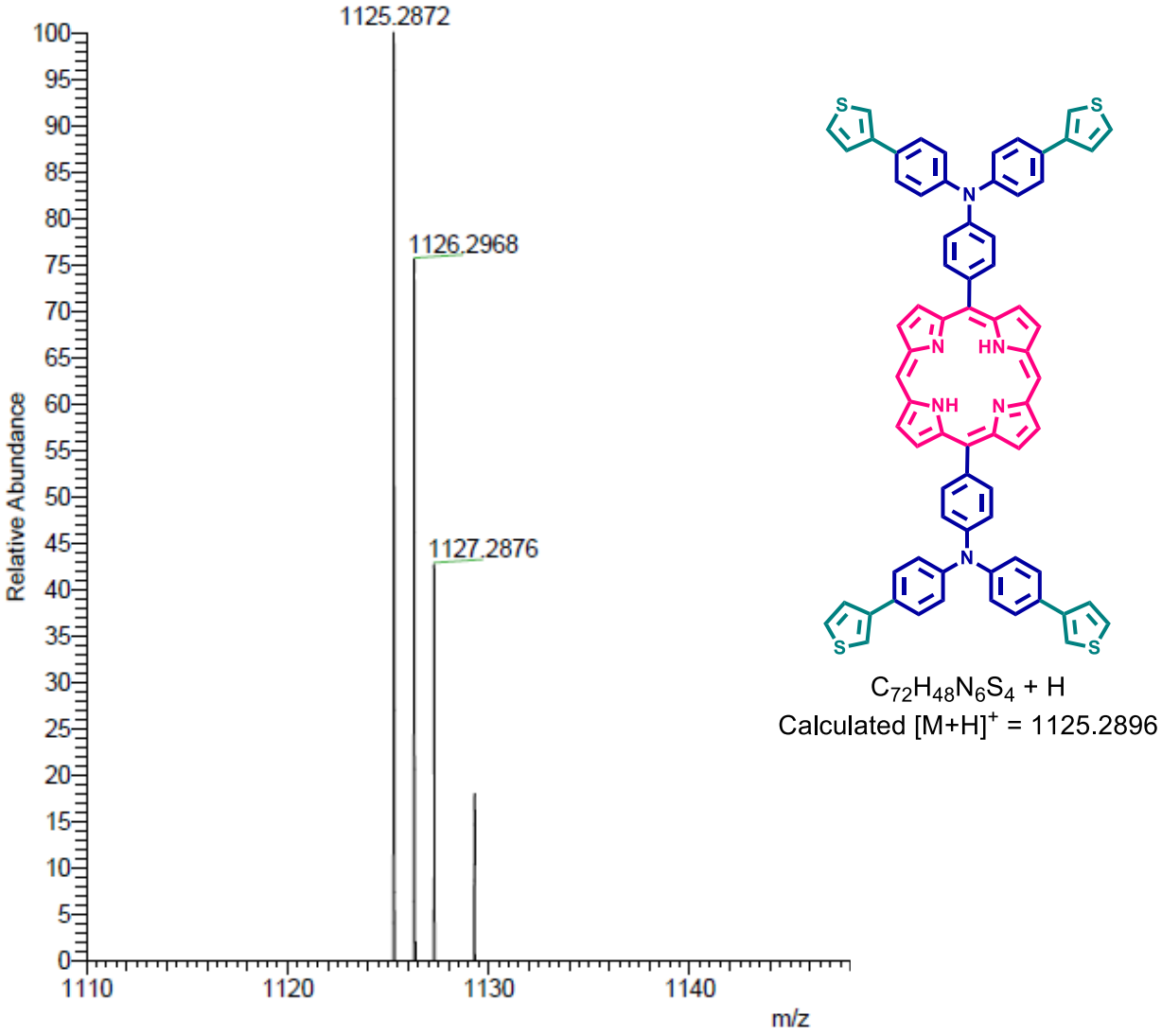


**Figure S21.** HR-Mass spectrum of **5a**

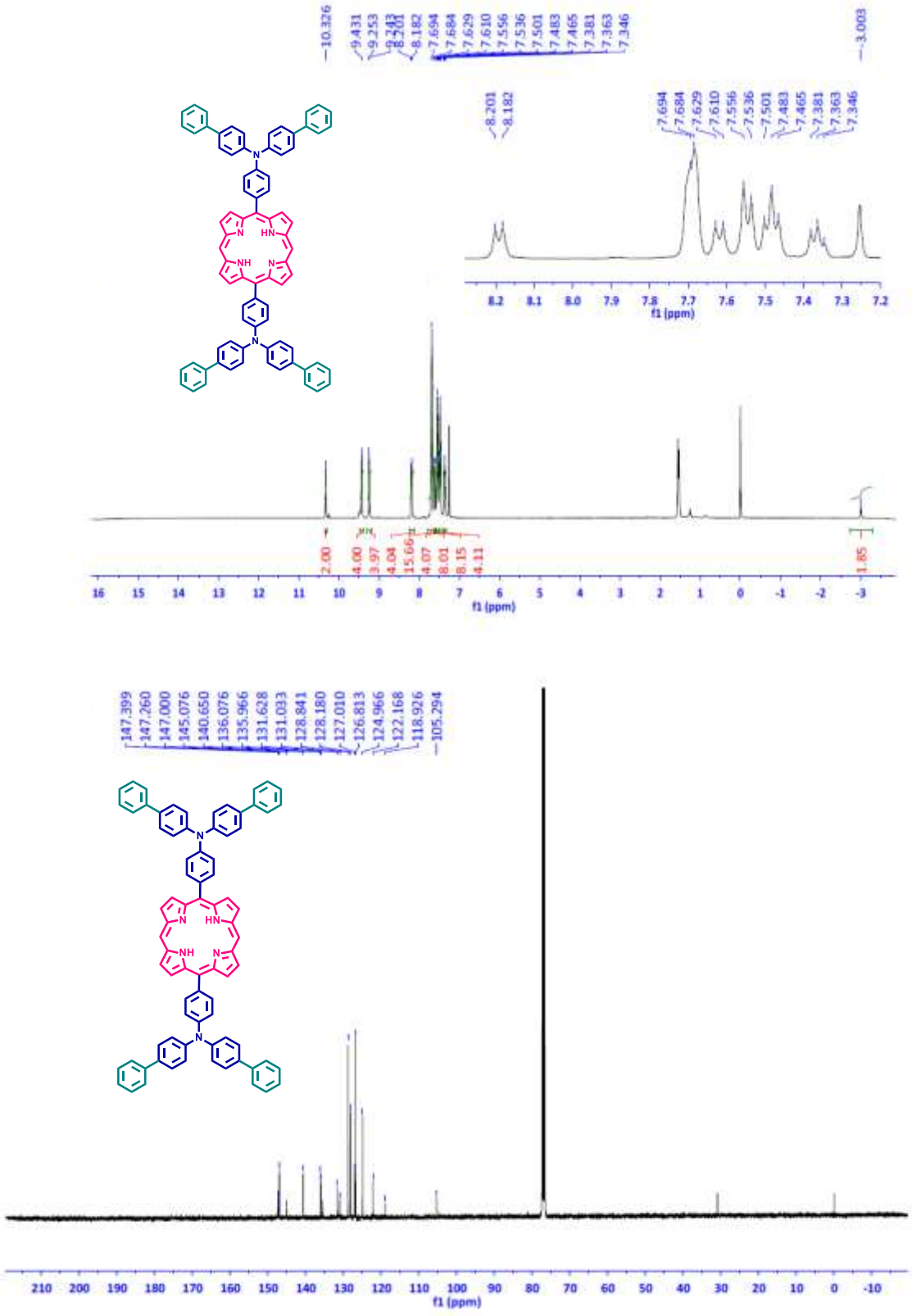


**Figure S22.** $^{1}$H NMR and $^{13}$C NMR spectra of **5b**

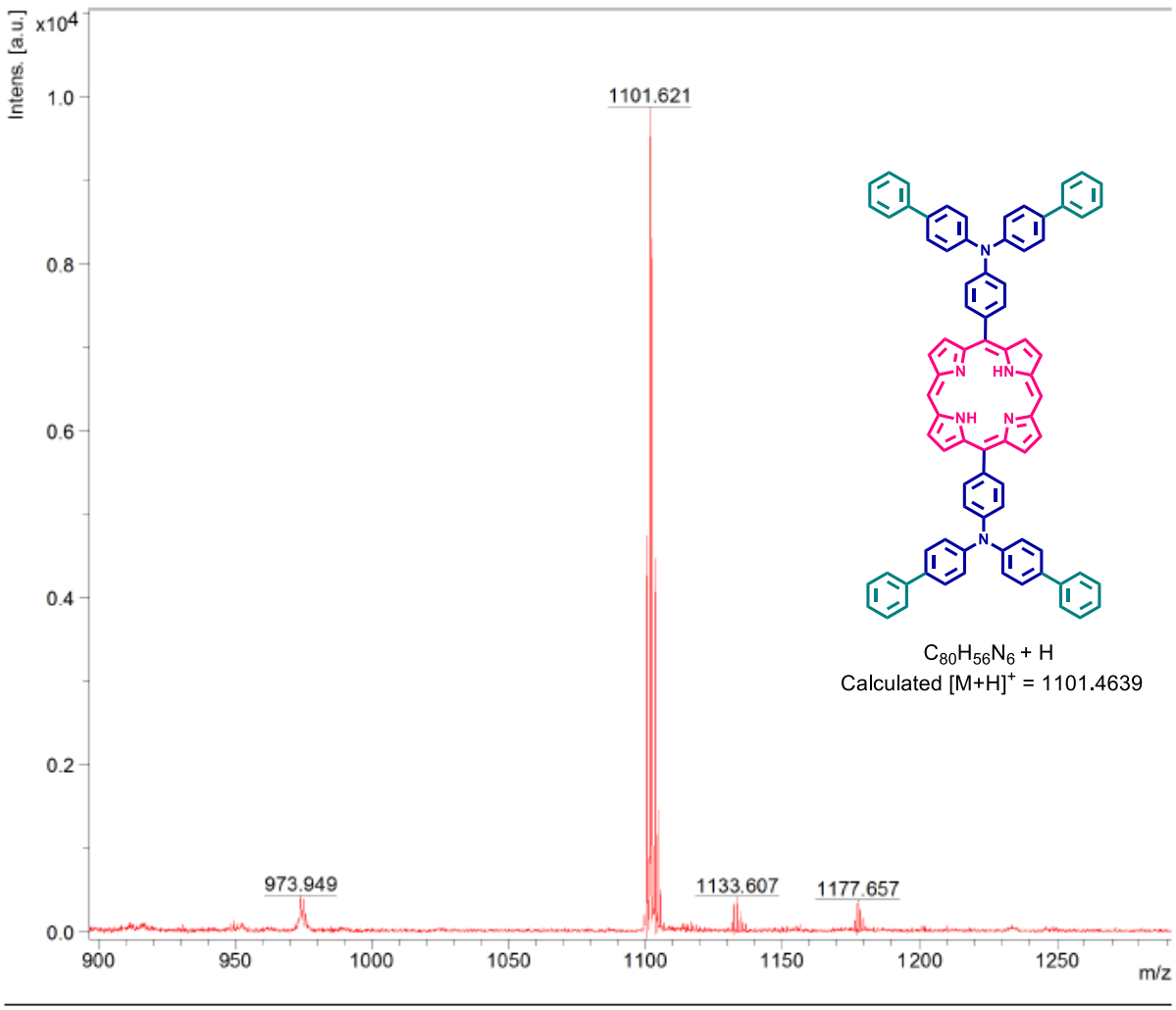


**Figure S23.** MALDI-TOF spectrum of **5b**.

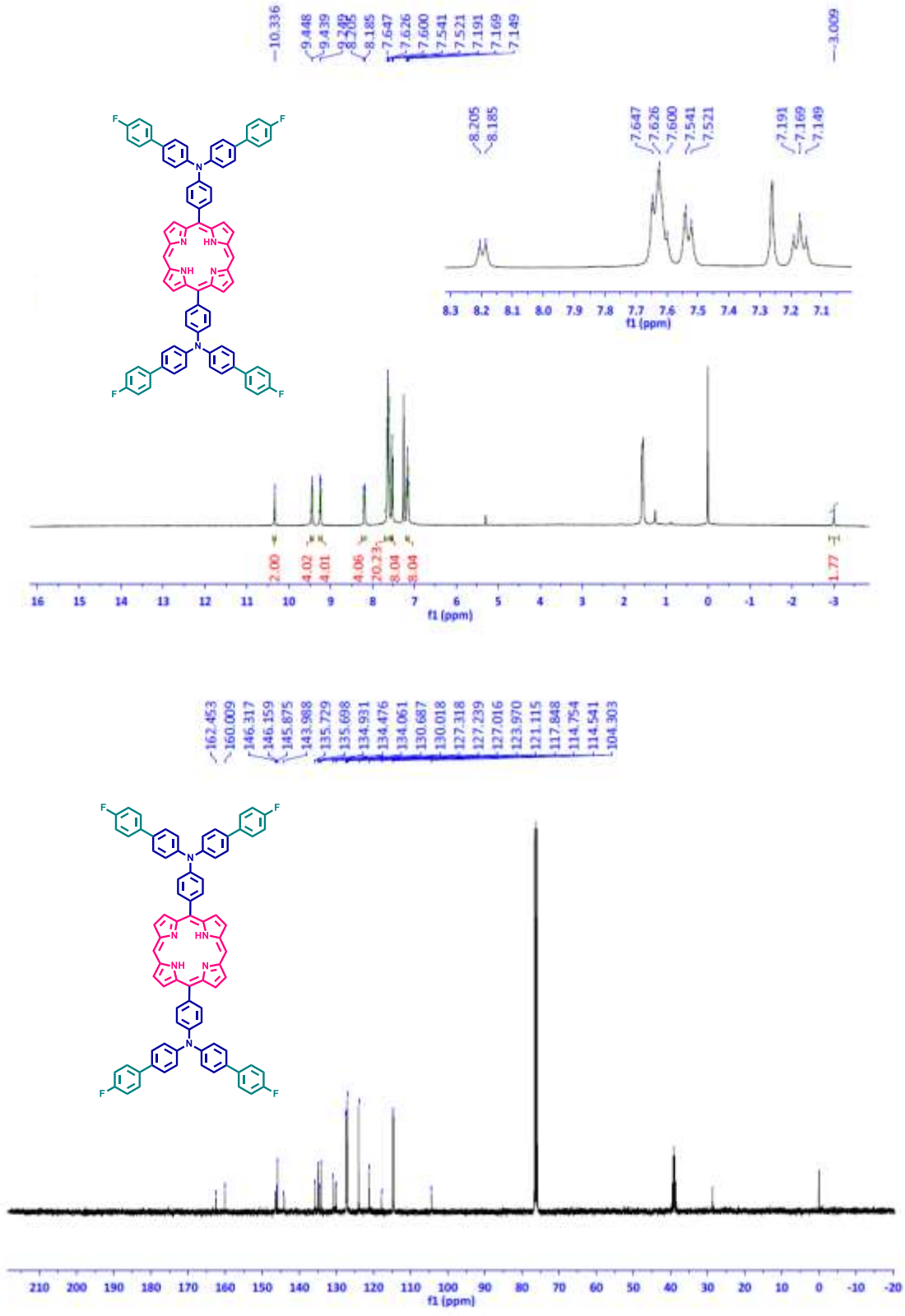


**Figure S24.**[1]H NMR and [13]C NMR spectra of **5c**.

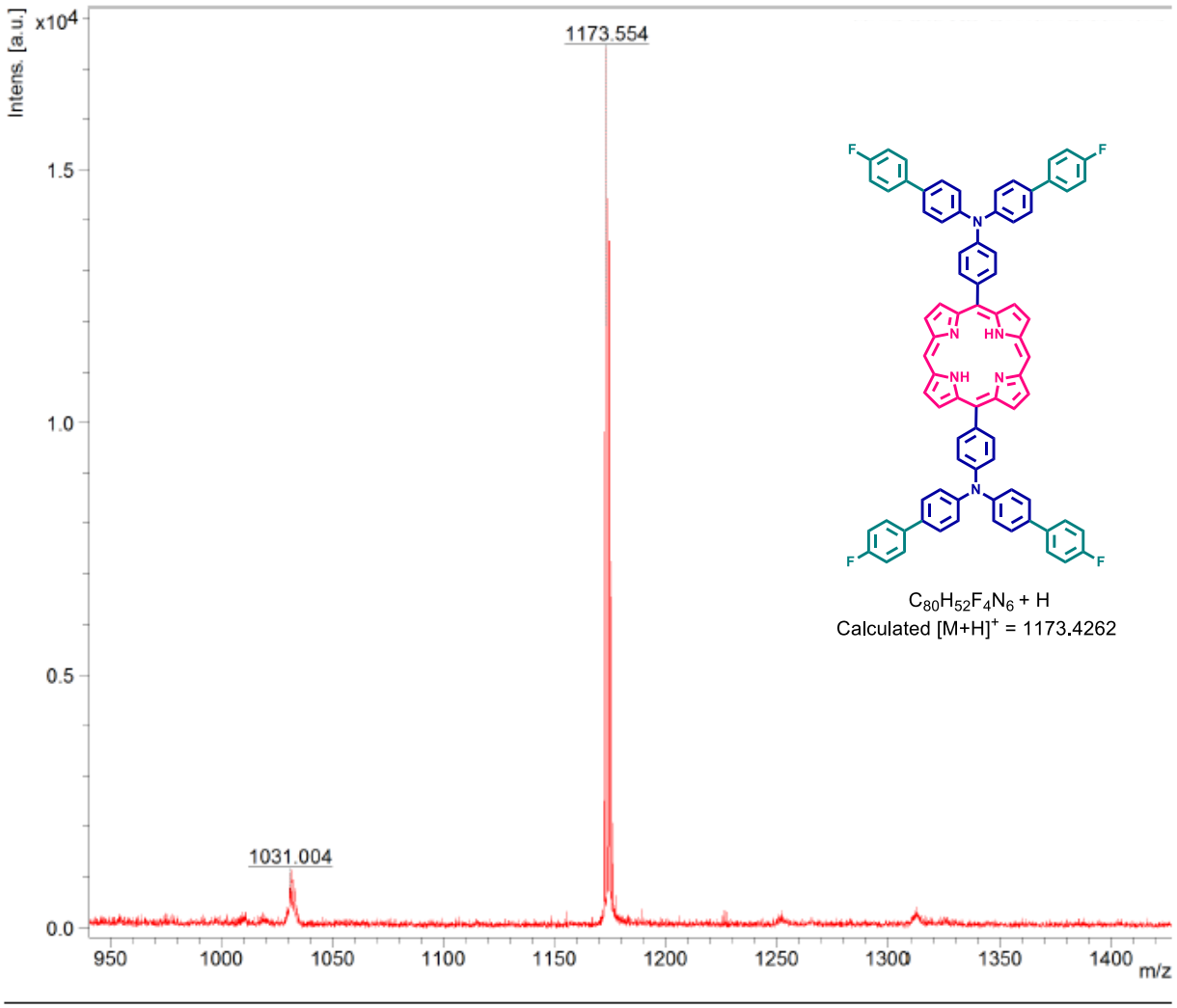


**Figure S25.** MALDI-TOF spectrum of **5c**.

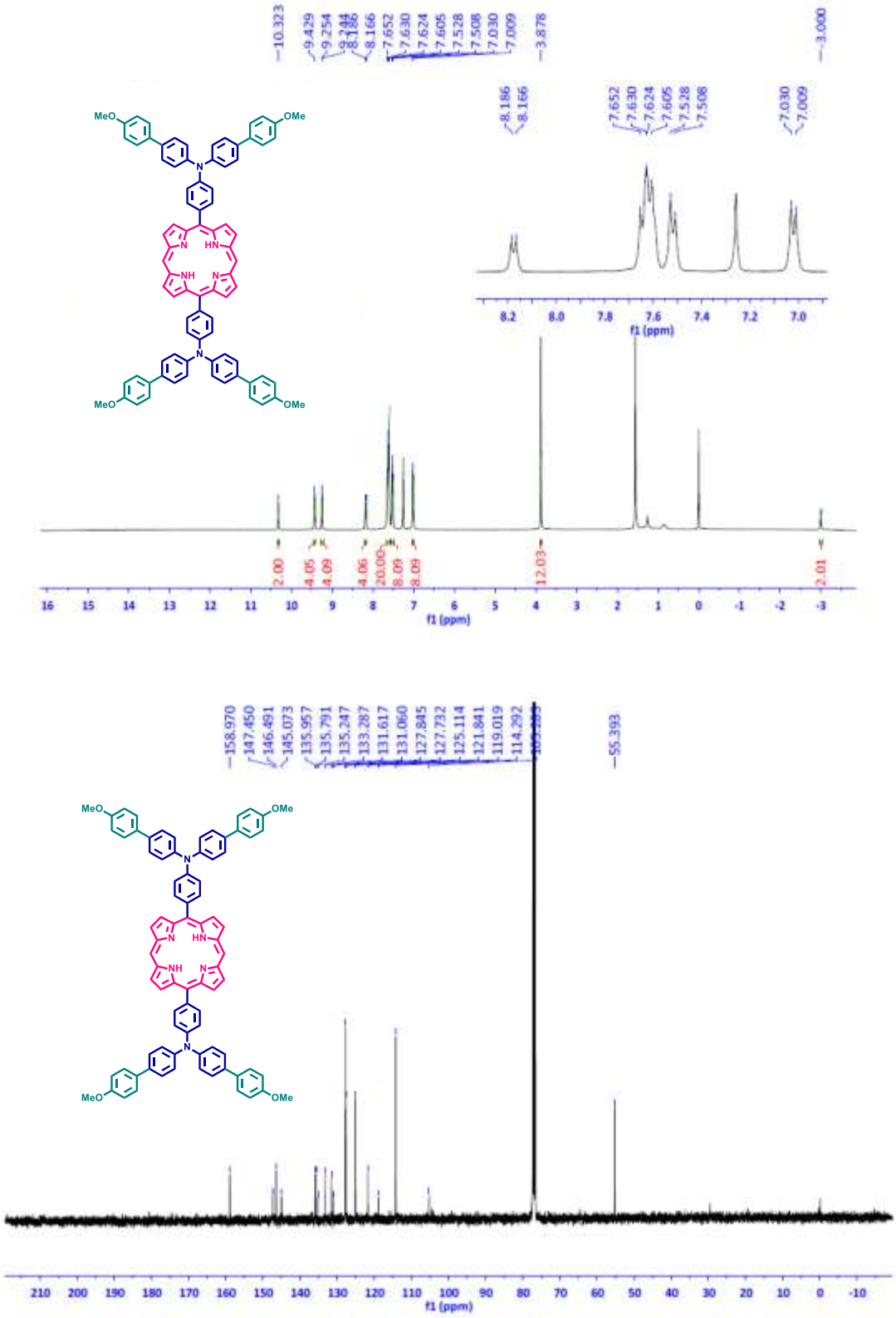


**Figure S26.** $^{1}$H NMR and $^{13}$C NMR spectra of **5d**.

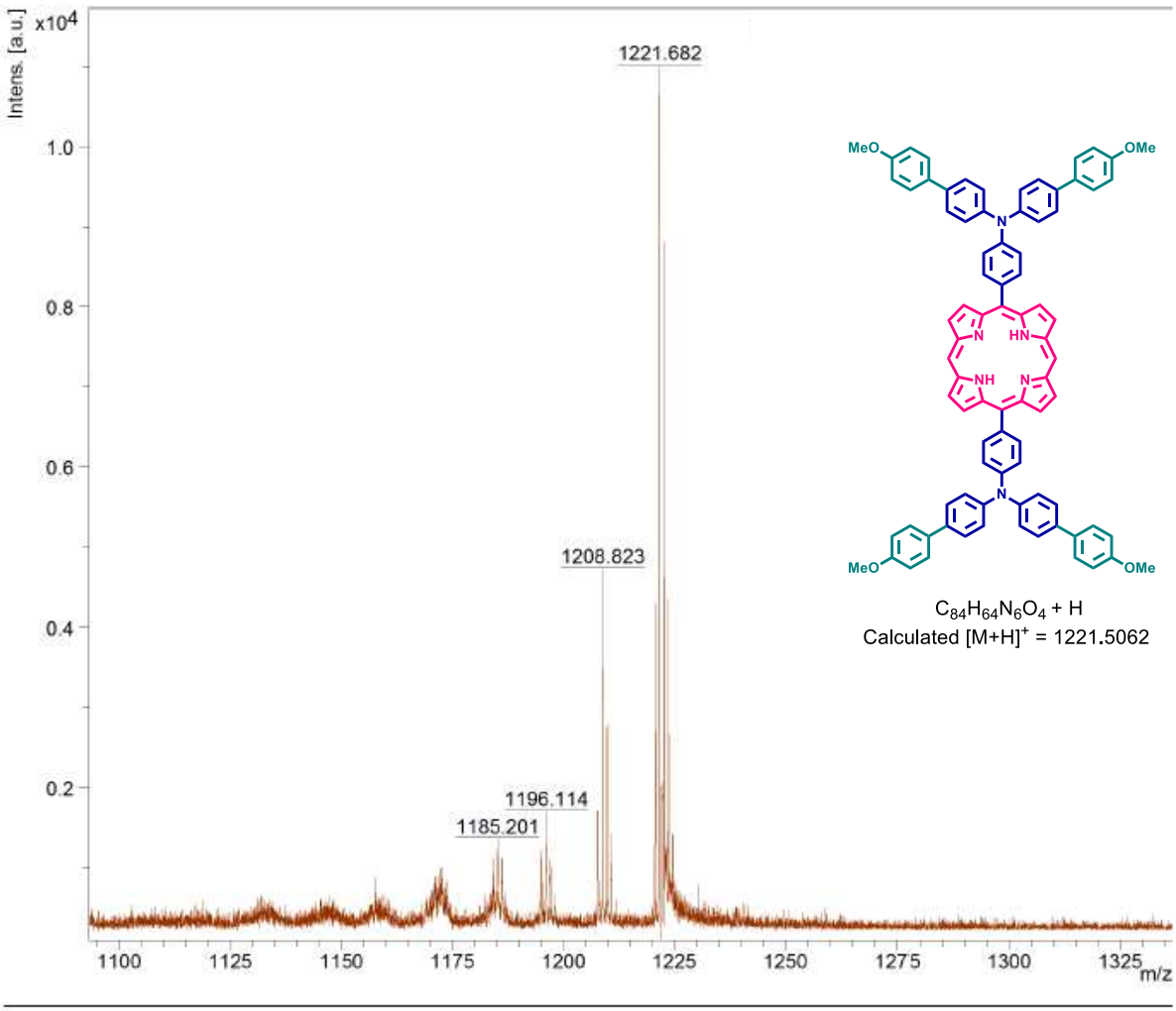


**Figure S27.** MALDI-TOF spectrum of **5d**.

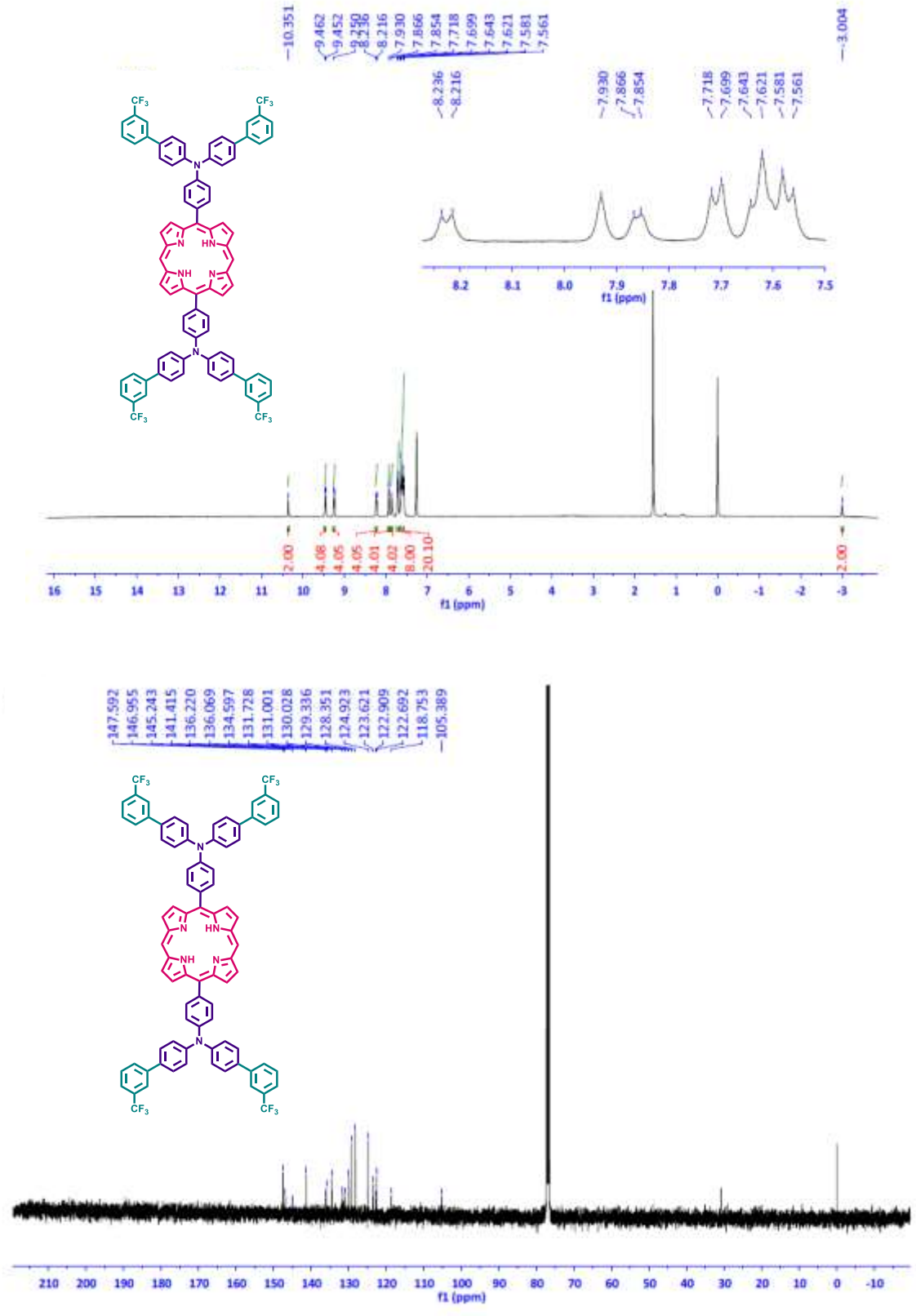


**Figure S28.** $^{1}$H NMR and $^{13}$C NMR spectra of **5e**.

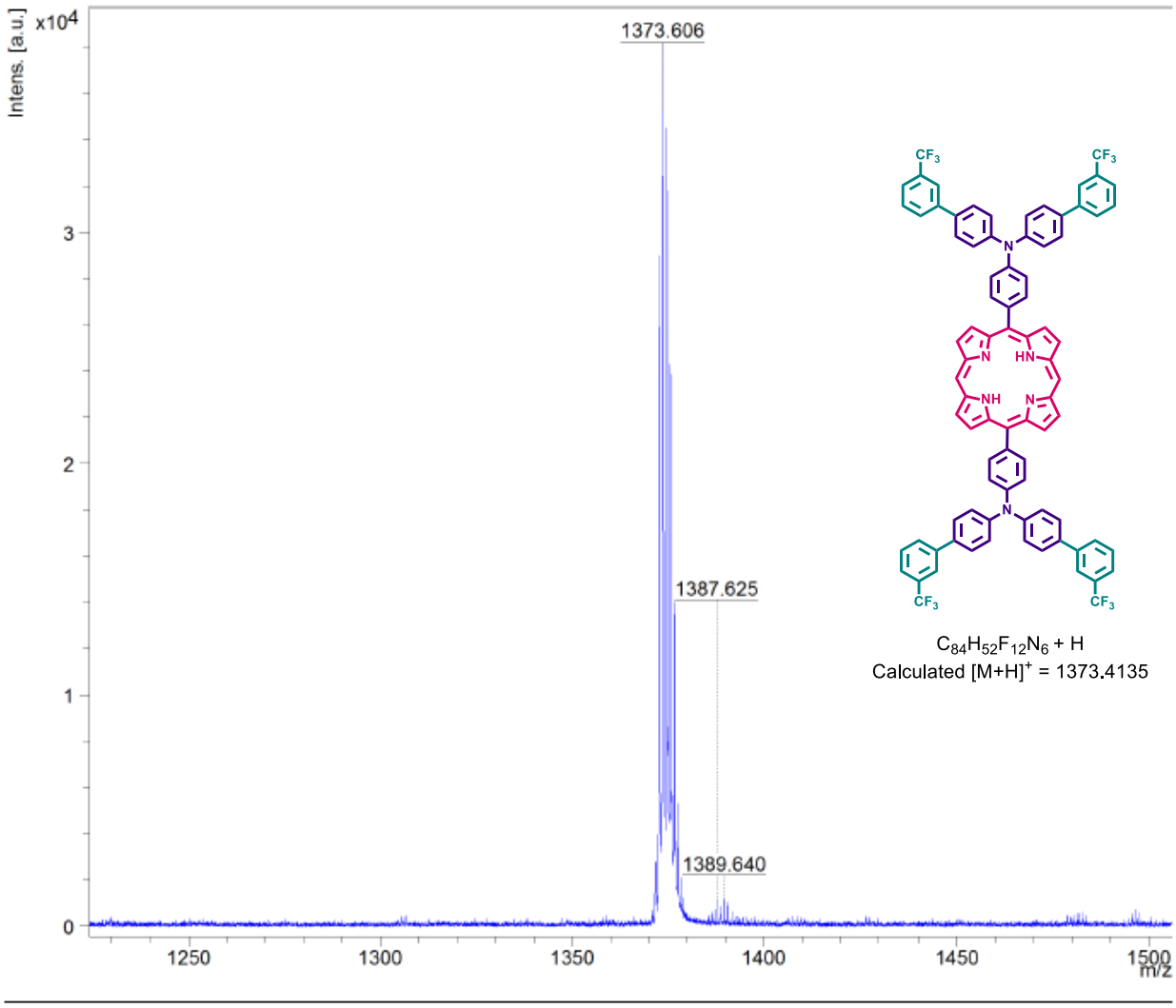


**Figure S29.**MALDI-TOF spectrum of **5e**.

## REFERENCES


(1) Lee, M. J.; Seo, K. D.; Song, H. M.; Kang, M. S.; Eom, Y. K.; Kang, H. S.; Kim, H. K. Novel D-π-A System Based on Zinc-Porphyrin Derivatives for Highly Efficient Dye-Sensitized Solar Cells. *Tetrahedron Letters*.**2011**, *52*, 3879–3882.

(2)Cheng, X.; Li, Q.; Qin, J.; Li, Z. A New Approach to Design Ratiometric Fluorescent Probe for Mercury(II) Based on the $Hg^{2+}$-Promoted Deprotection of Thioacetals.*ACS Applied Materials & Interfaces.* **2010**, *2*, 1066–1072.

(3) Frost, J. R.; Huber, S. M.; Breitenlechner, S.; Bannwarth, C.; Bach, T. Enantiotopos-Selective CH Oxygenation Catalyzed by a Supramolecular Ruthenium Complex.*Angew. Chem. Int. Ed*. **2014**, *53*, 1–6.

(4) Liu, B.; Zhu, W.; Wang, Y.; Wu, W.; Li, X.; Chen, B.; Long, Y.T.; and Xie, Y. Modulation of Energy Levels By Donor Groups: An Effective Approach for Optimizing the Efficiency of Zinc-Porphyrin Based Solar Cells. *J. Mater. Chem.* **2012**, *22*, 7434–7444.